FACULDADE DE ENGENHARIA DA UNIVERSIDADE DO PORTO

Structural Evaluation of a Motorcycle Frame

Carlos Filipe do Lago Vieira

Dissertation for Master's Degree in Mechanical Engineering

Supervisor: Mário Augusto Pires Vaz

Second Supervisor: Miguel Ângelo Nogueira da Costa Oliveira

October 2014

Structural Evaluation of a Motorcycle Frame

Carlos Filipe do Lago Vieira

Mestrado Integrado em Engenharia Mecânica

em09107@fe.up.pt

DEMec - Department of Mechanical Engineering
Faculdade de Engenharia da Universidade do Porto
Porto, Portugal

Abstract

This thesis presents a numerical analysis of a trail motorcycle frame. The frame is evaluated in different tests and its performance is evaluated. Solustions are also suggested for the current problems.

The finite element method analysis techniques were used for the solution of the problem. To that end, the program *ANSYS® Workbench 15.0* was used, for both modal analysis and static loads applied.

The model was analysed and its behaviour was evaluated in each of the cases. To improve its performance, an optimization of the frame model was done and suggestions were made.

Resumo

Esta tese apresenta a análise numérica de um quadro para um motociclo para trail. O quadro é avaliado em diferentes testes e a sua prestação é comentada. São também sugeridas soluções para os atuais problemas.

As técnicas de análise pelo método dos elementos finitos são aplicadas para a resolução do problema. Para tal efeito utilizou-se o programa *ANSYS® Workbench 15.0*, quer para a análise modal, quer para as solicitações estáticas.

O modelo foi analisado e o seu comportamento foi avaliado em cada um dos casos, tendo-se realizado uma optimização do modelo do quadro ou realizadas sugestões para o melhor desempenho do mesmo.

Acknowledgements

I would like to thank all my family specially my mother and my father who have given me unconditional support and guidance as well as my brother who taught me that giving up is not an option.

Also I want to thank all my friends that accompanied me all this years for the great moments and stories that we shared.

A special thanks to my flat mates who put up with me for four years for their never ending support and understanding.

I would also like to thank Professor Dr. Mário Augusto Pires Vaz for the support and availability during the course of this thesis.

Carlos Filipe do Lago Vieira

"I have not failed.
I've just found 10,000 ways that won't work."

Thomas A. Edison

Contents

List of Figures

List of Tables

Abbreviations and Symbols

σ_y	Yield Stress
σ_u	Ultimate Tensile Strength (UTS)
ρ	Density
ø	Diameter
APDL	ANSYS Parametric Design Language
CAD	Computer Assisted Design
E	Young Modulus
FEM	Finite Element Method
RX	Rotation over X axis
X	X axis
Y	Y axis
Z	Z axis

Chapter 1

Introduction

This thesis was done as the final dissertation of the author's Master Degree in Mechanical Engineering conducted in Faculdade de Engenharia da Universidade do Porto .

The project appeared after the contact of AJP Motos with Faculdade de Engenharia da Universidade do Porto , in order to study a motorcycle frame using the finite element method. This was a challenge that the author was keen on taking due to his interest in being involved in a development project such as this.

A motorcycle has as defining characteristics its high power-to-weight ratio, the low fuel consumption and its nimbleness (mainly provided by its thin body shape). For this reason the lightness of the motorcycle is a very desirable feature. To accomplish this, lighter metallic alloys, such as aluminium, are employed in the construction of motorcycle frames.

The motorcycle frame is the structure that supports major motorcycle components like the engine, front and rear suspension, fuel tank, etc.. It is also the element responsible for the stiffness of the whole vehicle and how it handles and reacts.

AJP Motos is a Portuguese company operating since 1987, on the off-road motorcycle segment. Nowadays AJP Motos range comprehends 3 models, which were developed for recreational Enduro riding, with the ability to be used in races and in daily transportation.

AJP Motos intends to widen its range, by entering in different segments. The company is currently studying a new model designed for the trail segment but better adapted to urban driving.

For this reason, an analysis of the current design of the frame is needed.

1.1 Given Objectives

As in any other project, objectives were set up before the start of the project.

For the correct analysis of the frame, its connections and constraints need to be understood. Also the critical loads that the frame is to be subjected need to be determined and comprehended.

The current frame needs to be analysed using FEM software and its results should be completely understood and commented.

The structure needs to be lightweight, to address the power-to-weight characteristic of motorcycles, but stiff, to provide good handling to the vehicle.

With the results in hand, improvements should be suggested and tested with FEM software.

All of this should also be based on previous works (such as books, thesis, etc.) as information is valuable so that mistakes are avoided and improvements are made.

An experimental test of the prototype, in the lab and on the track, should also be made in order to validate the results and refine the analysis model.

1.2 Methodology Applied

For the solution of this work the Finite Element Method was applied in order to study the stiffness of the frame and possible failures in service, identifying critical points.

However, to make this possible, the motorcycle frame had to be drawn using a CAD software (*Pro/ENGINEER*® and *Solidworks*®) and then the geometry had to be imported into the FEM software (*ANSYS*® *Workbench 15.0*).

Afterwards the connections between the different parts, the boundary conditions, had to be implemented in the model.

With the basis of the work set up, it was needed to create some load cases that could translate the normal usage of the motorcycle as well as the properties of its frame.

With the informations collected, improvement suggestion should be made and tested so that the final product confers comfort and safety to its rider.

1.3 Outline of the Thesis

This thesis is split in 6 chapters whose content is briefly explained in the following points.

Chapter 1 - A simple introduction to the thesis with a brief description of its objectives and outline.

Chapter 2 - This chapter contains a brief history of the motorcycles and different types of

frames are also explained, showing some examples. The trail motorcycle is characterized and a short historical background is presented. Given that this work was requested by AJP Motos, the history of the company is also cited. Lastly, the Finite Element Method, method in which the majority of this thesis is based, is described.

Chapter 3 - The motorcycle frame is dissected in this frame and its different parts and materials are explained. The importance of each individual part on the motorcycle is addressed, as well as its defining characteristics and construction method.

Chapter 4 - Various cases of static loads, applied to the frame in order to exemplify its normal usage, are set up. The results, obtained through *ANSYS® Workbench 15.0*, are also shown and interpreted.

Chapter 5 - The natural frequencies of the frame and swing-arm are retrieved using *ANSYS® Workbench 15.0*. The results are compared with a previous work done for the same company and are defended.

Chapter 6 - At last, the final considerations about this thesis are done. The accomplishment of the objectives is reflected on as well as the problems and obstacles found during the process of this thesis. Future works are also suggested so that a further optimization of the motorcycle can be made.

Chapter 2

State of the Art

In this chapter the history and evolution of the motorcycle as well as the different types of chassis of these vehicles is addressed. This approach helps understanding the different types of chassis and its properties so that an accurate analysis and further optimization can be achieved.

There is also an insight about the company who is building the motorcycle where this chassis will be implemented.

The main requirements of actual motorcycle design are also presented.

2.1 Motorcycle History

2.1.1 Early Days

The origin of motorcycles dates back to 1868 when Sylvester Howard Roper made a steam-powered bike (Figure 2.1), achieving the goal of building the self-propelled bicycle. [1]

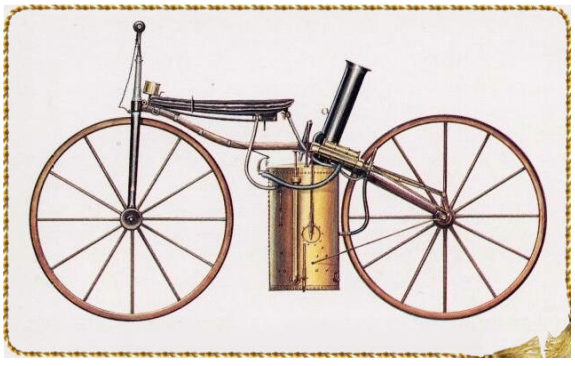

Figure 2.1: 1867 Sylvester Howard Roper Steam Velocipede [2]

However, the first petrol-based motorcycle (Figure 2.2), was only created in 1885 by the German inventors Gottelieb Daimler and Wilhelm Maybach, thus creating the first ever motorcycle (motorized bicycle). It was driven by a single-cylinder Otto-cycle engine mounted in the center of the machine and had a wooden chassis, wheels with iron rims and spokes made of wood. Even though the official name of this motorcycle was Daimler Reitwagen, it was known as "Bone-Crusher" or "Bone-Shaker" for its jarring ride and the tendency to toss their riders. [3]

This vehicle set the basis for today's motorcycles, since the transmission system as well as the controls positioning used are close to that we are used today. For instance, the power was transmitted to the rear wheel using a belt mounted in the crankshaft that drove a countershaft pulley, this last one was used to drive a gear built in the spokes of the wheel. The handlebar was clamped into a metal linkage that attached to front fork, thus allowing the driver to steer. The clutch and the rear brake were engaged simultaneously by turning a twist-grip on the right hand end of the handlebar. It is impressive to see how much of these systems persisted or reappeared on today's motorcycles. [4]

Figure 2.2: 1885 Daimler Reitwagen [5]

In the beginning of the development of the motorcycle, various solutions were tried for the engine positioning. The actual solution was only achieved in the beginning of the 20^{th} century, putting the engine on the inside of the frame. [6]

The engines were also a part of great discussion. The manufacturers experienced with different number of cylinders and dispositions, achieving the conclusion that an even number of cylinders offered a smoother ride and could reduce vibrations. There was also the two stroke engine in the equation but, even with its superior power-to-weight ratio, it became unused and banned from production due to the high emissions caused by the fuel-oil mixture being burnt. [4]

In 1889 the air-inflated pneumatic tyre is invented by John Boyd Dunlop, opening a path to smoother rides in motorcycles and cars alike. [7] This feature was included in the 1892 motorcycle designed by Alex Millet which, even though it's design was still that of a safety bicycle, had a rear wheel mounted 5 cylinder rotary engine where the cylinders rotated with the wheel, while the crankshaft formed the rear axle.

The first manufacturer to be able to mass produce motorcycles was DeDion-Buton in 1895. This was achieved with the introduction of a small, lightweight 4 stroke engine that could generate half a horsepower. Setting the basis for the actual motorcycle production. [3]

Based on this design, the Indian Motorcycle® Company begins the production of their 1,75 hp motorcycle (Figure 2.3). These Indian motorcycles were the world's best selling motorcycle until the 1st World War. [7]

Figure 2.3: 1901 Indian Motorcycle [8]

2.1.2 The War and the Motorcycle

In the beginning of the 1st World War, in 1914, the motorcycles owned the roads since they were such reliable and independent vehicles. Their utilitarian nature made them also a great asset for the war, where motorcycles were used extensively as reconnaissance, message delivery vehicles and in some cases to engage in combat (Figure 2.4). It was estimated that the U.S.A. Army used around 20.000 motorcycles in the war (most of them being Harley-Davidsons). By the end of the war, Harley-Davidson was the biggest motorcycle manufacturer in the world.[3]

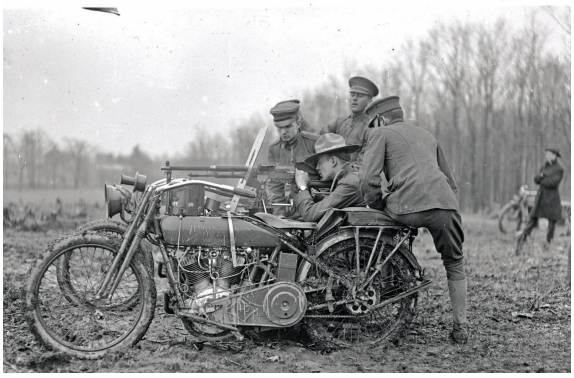

Figure 2.4: WWI Harley-Davidson Motorcycle [9]

When the war ended, the world was more motorized than ever, which lead to a boom in the motorcycle industry in 1920. At this time the manufacturers BMW and Moto Guzzi enter the market, however, with the Great depression, many motorcycle manufactures are forced to go out of business. [7]

After World War II, the European companies registered another boom in sales. Also at this time the Japanese companies start the manufacturing of motorcycles, having built the first Honda in 1947 (Figure 2.5) and the first Kawasaki in 1949. [10]

Figure 2.5: Honda Model D: first ever Honda motorcycle [11]

2.1.3 Motorcycles Nowadays

In nowadays world, motorcycles present a distinct function depending on the part of the world they are in. In the developed world, motorcycles are mainly a luxury good, used mostly for recreation, as a lifestyle accessory, or a symbol of personal identity, while in developing countries motorcycles are overwhelmingly utilitarian due to lower prices and greater fuel economy.

What makes it so popular are its low consumption, the high power-to-weight ratio and its nimbleness. In a world with cities constantly packed with traffic jams, these are desired characteristics in a vehicle.

The controls used in the motorcycles nowadays have remained essentially unchanged since the 1920's and are practically identical for all the motorcycles manufacturers today. The last big change in the motorcycle controls was done, reliably, in 1965 with Honda models, which included electric starters. This had remained the same since the introduction of the kickstarter in 1909 by Alfred Scott on his 333cc motorcycle (which became a standard only two years after). Also, modern motorcycles have all converged to an essentially standard wheel system consisting of tubeless pneumatic tires mounted onto cast aluminium wheels, with a separate disc brake controlling the front wheel and rear wheels. However that is where the similarities end. There are many different motorcycle engines, transmissions and suspensions systems, all of which are to correspond to the styling and performance characteristic that most closely matches their motorcycle type. The various types were created so that the performance requirements of the riders were fulfilled. [4]

2.2 Frame Designs

The frame of a motorcycle it's what holds the mechanical components of the motorcycle together and it can be made from a variety of materials, including steel, aluminium and magnesium.[12] This part has to combine performance with practicality and has to be an ideal structure that doesn't flex, weights as little as possible and has to be accurately built so that the motorcycle's manoeuvrability is good.

To achieve a precise steering the chassis must resist bending and twisting sufficiently so that the steering axis remains in the same plane as the rear wheel, regardless of the loads imposed by the transmission, bumps, cornering and braking. Good handling also translates in less user fatigue, because the effort needed to ride the bike is minimal.

Early motorcycle frames can trace their roots back to bicycles. They were little more than a simple steel-tubed diamond with an engine that hung off it. As power outputs increased and speeds went up, primitive suspension systems began to appear. The stresses going into the frame increased and designers had to add more material to stiffen them, preventing flex and movement that cause instability. [13]

The frame has a static and a dynamic function. The static part concerns supporting the weight of the rider (or riders), the engine and transmission as well as all the other necessary accessories, such as fuel and oil tanks. As for the dynamic function, the frame must confer precise steering, good road holding and comfort, while working in conjecture

with the rest of the rolling chassis. The motorcycle's engine can also be a stressed member of the chassis and can have rigid or flexible mounts.

As for a good evaluation of the structure's performance there is the stiffness to weight ratio, also referred to as structural efficiency. [14]

There are a variety of frame types which will be described on the following sub-chapters.

2.2.1 Tubular Frames

The tubular frames were the first frames introduced to the motorcycle world since they derive directly from the bicycle frame.

Before the adoption of rear springing, most frames were diamond shaped. This design also suited the tall single cylinder engines used at the time.

After the diamond shaped frame came the cradle frame (Figure 2.6). This configuration presented the bottom ends of the single front and seat tubes spaced farther apart and rigidly connected by a brazed-in engine cradle, from the rear of which the tubes reached upward to the wheel-spindle lugs.

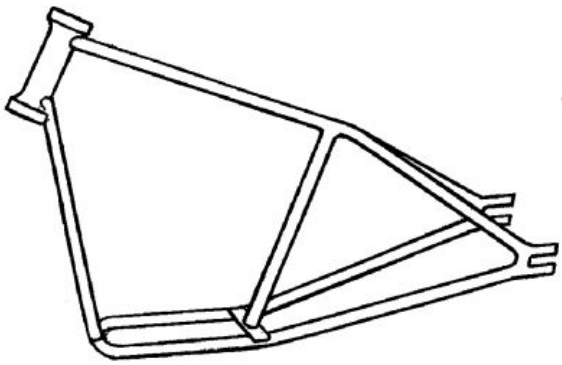

Figure 2.6: Cradle frame [14]

The duplex cradle frame was a straightforward development of the single cradle frame. This design had the cradle tubes extend upwards towards the steering column. Both this designs suited well the upright single cylinder engines that were used in the early days.

The torsional and lateral stiffness seem to have been given a low priority in these early designs but there were some efforts between the wars to ensure both the torsional and lateral stiffness through the triangulation of the frame structure. [14]

2.2.2 Trellis Frames

This type of frames offer extremely high structural efficiency, even so, few of the major manufactures adhered to them. This may be due to the rather high cost of the frame, since the shape and size of the most popular engines require a wide and complicated structure.

When building these frames it is critical to watch out for the vibrations produced by the engine unbalanced inertia forces in long tubes of small diameters, as, at a critical frequency, it can cause resonance. A solution is to shorten the tube or increase the diameter. Also, note that this is not unique to the trellis frames as it can happen in any design given it has long and thin members. [14]

The fabrication of these frames involves welding and precise jigging. The lightweight property of this structure as well as the rigidity it has, confers the high structural efficiency referred before. [15]

Figure 2.7: KTM 200 Duke Triangulated Frame [16]

2.2.3 Tubular Backbone Frames

As the name indicates the defining characteristic of these frames is the tubular backbone. This frame doesn't have a high acceptance despite having a good structural efficiency (given that the diameter of the backbone is large enough).

This kind of frames also have difficulty accommodating bulky engines. Ideally the tube should be straight and connect the steering head to the rear suspension pivot, but in practice this is seldom possible. With flat or medium sized engines, however, it is usually feasible to bring the backbone to within a few centimetres of the pivot and bridge the gap with a welded-up box section. Another way to gain the necessary engine clearance is to bend the tube, in this situation, some designers, use the engine as a structural member to

Figure 2.8: Kawasaki Z800 Tubular Backbone Frame [17]

confer higher structural efficiency. An efficient frame can also be produced using a high-level straight backbone and linking it to the engine and rear-suspension pivot by means of an arrangement of smaller diameter straight tubes. [14]

2.2.4 Fabricated Backbone Frames

This construction makes for rigidity and low production cost, though the high initial tooling outlay rules it out for small production and special runs. The final product is also heavier than an equally rigid tubular backbone because of the inevitable excess metal in areas of low stress.

The most popular design for a fabricated backbone is a T-shaped structure comprising left and right steel pressings united by spot or electric-resistance welding. [14]

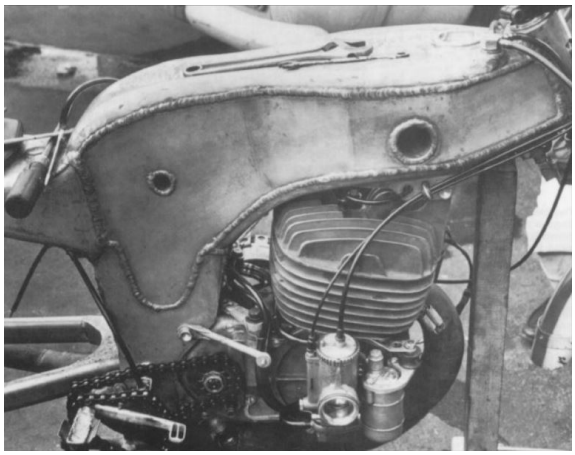

Figure 2.9: Fabricated Backbone Frame from the 1960s 250 cc Ossa GP [14]

Due to the weight of this kind of chassis, they have a low structural efficiency values (ratio between the mass a structure can hold and the mass of the structure), even though the frames provide high rigidity. [15]

2.2.5 Monocoque Frames

These frames are similar to the aircraft frames that have stress at the skin. Even so, they are much less amenable to build for a motorcycle than for a car or a plane, due to the irregular shape and the need for several cut-outs. [14]

Monocoque frames present, as mentioned before, stress at the skin but they also have an underlying rib structure.

When made out of composite materials, such as carbon fiber, this style of frames present a very high structural efficiency. [15] One of the downsides of this frame is the poor accessibility for maintenance, making it difficult and slow. [14]

Frames with this design are used almost exclusively on specialized competition bikes and are not a good choice for street bikes. [18]

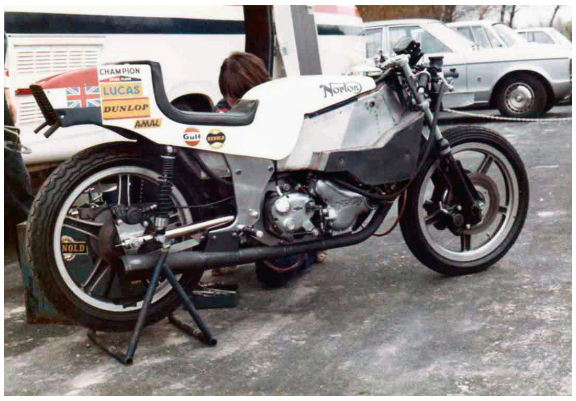

Figure 2.10: 1973 John Player Norton monocoque chassis [19]

2.2.6 Twin-spar Frames

This style of frames, also know as Perimeter or Beam Frames, is nowadays the style used in most top of the range sports bikes and racers. It is used even in off-road and trial bikes.

It is mostly made of aluminium and comprises of two beams running each side of the engine/gearbox unit, joining the headstock to the swing-arm pivot mountings. These side beams have generally got bigger with time to provide increased stiffness. Three methods have been employed for the construction of the side components: extruded tube (often with internal ribbing), fabricated from sheet and castings.

The structural efficiency of this frame is not particularly good, however, given enough metal it can achieve a better stiffness even for racing duties. If made of aluminium, this type of construction method is not one that gives a particularly light frame. However, if made of steel, as most other frames are, it would seem positively heavy.

Figure 2.11: Twin-spar frame from a Yamaha R1 [14]

Throughout history, very few frames were built with structural efficiency as the primary objective, as other properties take preference. Manufacturers are more concerned with success on the race track and in the showrooms, and in that aspect the twin-spar frame has to be considered as successful as the multi tubular was a few decades ago.

This design offers considerable packaging advantages, especially in the racing context as it allows much easier access to work on the engine. The elimination of the down tubes and the lower cradle also sets free valuable space in the area needed by exhaust and cooling systems. [14]

2.2.7 Structural Engine

Using a structural engine is not a type of frame design but it most certainly is a way of complementing one. Building a frame contemplating a structural engine is probably the most efficient way to build a bike with a large engine.

The principle here is to use the inherent stiffness of the engine gearbox unit to provide the major support between the steering head and the rear-suspension pivot. This allows for increased stiffness without having added weight. [14]

2.3 Trail Motorcycle

The trail motorcycle or dual-sport motorcycle is a type of motorcycle designed to work well both on road and off-road. It is the ideal motorcycle for those who want to experience

a little leisure off-road but still be able to drive it back home through the paved motorway.

These motorcycles are bigger than their usual pure off-road counterparts therefore they are more comfortable to be ridden on asphalt.

In order to achieve this, it is required that the chassis is strong enough to absorb the impacts and resist the continuous use of the motorcycle off-road while cushioning the undesired vibrations during a casual ride home.

The dual sport motorcycle has been around forever. During the 1950's and 1960's riders would go "Stump Jumping" with their Harley, Triumph or BSA. After that, in the 70's, as the manufacturers started building bikes more specialized for what they were designed the dual sport motorcycle faded. [20]

The first "proper" motorcycle of this kind appeared on 1980 when BMW unveiled its R80 G/S model (Figure 2.12). A vehicle that looked like a dirt bike but had a 800cc flat-twin motor from a streetbike. [21]

Figure 2.12: 1980 BMW R80 G/S [22]

2.4 The Company: AJP Motos

In 1981, at only 22 years old, Antonio Pinto opened a Motorcycle Repair and Modifications shop. Later in 1987, AJP was founded and presented its first creation, the ARIANA 125cc, equipped with a 2 stroke Casal engine, named after Antonio Pinto's daughter born in that same year. This motorcycle was produced within a limited series of 25, but it had already adopted many original technical solutions that were further explored in future models. In 1991, AJP established a partnership with Petrogal (Currently Galp Energia), whose most noteworthy outcome was the development of the AJP Galp 50, and secondarily developed of a whole range of synthetic oils for 2 stroke engines, tested Unleaded gasoline with additives.

From 1991 to 2000, AJP participated in the National Championships of Enduro, winning five titles in a row from 1996 to 2000. AJP also participated in the National Off-Road Championships, with victories in 1996, 1997 and 1999. 2001 represented a turning point for AJP: a new motorcycle, the AJP PR4 125, boasting a 4-stroke engine, was launched into the market. Yet again, innovation is present in the fuel tank positioned underneath the pilot's seat. (an innovative feature still present in today's models), this disposition allows for a more aggressive behavior by lowering the gravitational axis of its motorcycles. The AJP PR4 125cc marks the beginning of AJP's export activity, with the very first units being sent to various European countries. France, Germany and England were the first countries to buy AJP motorcycles.

In 2003, AJP relocates to a new facility in Lousada and In 2004 introduces a new version of PR4 with a 200cc 4-stroke engine. This model shares the same components as the 125, though offering a more able and potent engine. Thanks to this model, AJP expanded it's business into Spain, Poland, Italy and Greece as well. In 2007, the AJP PR3 200 MX is launched. The model introduces a new concept of frame developed in-house, with double aluminum spars. This solution allies the lightweight to a simpler production at the same time revolutionized the motorcycle's visual aspect, bestowing a modern and attractive design. A PRO version follows, with a set of evolved suspension. Weighing only 89 kg, the PR3 ranks as the lightest four-stroke 200 cc Enduro bike in the world. The short wheelbase gives the model an agility of a trials bike but it is still a full size bike. A 69x53 mm bore and stroke gives 13.2 kW (19 bhp) of smooth power with a linear delivery.

At the end of 2008, sales take off for the homologated versions of the PR3 series, with a 125cc engine, and the 200cc one at the beginning of 2009. In 2009, AICEP Capital Global becomes a partner of the project. Its involvement is intended to provide the company with the necessary means for the development of its expansion plan of activities. At the end of 2009 AJP's releases its most ambitious project yet, the PR5 (Figure 2.13). The PR5 is fully homologated in the European market and the fuel-injected 250 cc engine is quick - but still in a 100 kg full-size package. The PR5 specifications include most of the technology developed by AJP over the years.

Praised by the specialized media worldwide, the PR5 opened new markets for the company including Japan and Brazil. What sets AJP apart from other manufacturers is the fact that Antonio Pinto himself hand-checks each and every bike that leaves the factory. According to Pinto AJP designs off-road motorcycles that can get from one point to the other in everyday activities but can ultimately give its rider a race-like experience if so desired. [23]

Figure 2.13: AJP PR5 Enduro [23]

2.5 Finite Element Method

Much work is involved before the fabrication of any advanced engineering system begins. This is to ensure the workability of the finished product, as well as cost effectiveness. For this reason, nowadays, the Finite Element Method (FEM), is indispensable in the modelling and simulation of advanced engineering systems in various fields.

The usual process followed in the development of these systems is explicit in figure 2.14. This process is usually iterative so some procedures are repeated multiple times based on the results. The main objective is to achieve optimal performance with the lowest cost possible for the system to be built. [24]

In structural engineering, the FEM has as an objective the determination of the stress and strain states of a solid with arbitrary geometry subjected to exterior actions with given boundary conditions. [25]

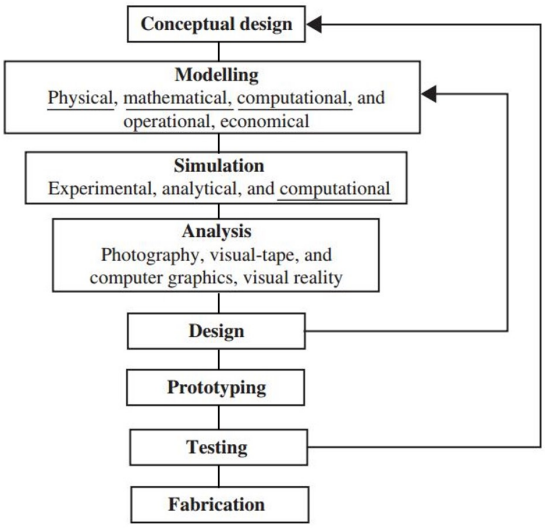

Figure 2.14: Process leading to fabrication of advanced engineering systems [24]

The FEM was first used to solve problems of stress analysis, and has since been applied to various other problems like thermal analysis, fluid flow analysis, piezoelectric analysis, and many others. The basis behind them all is the same, since the analyst seeks to determine the distribution of some field variable (like the displacement in stress analysis).

It is a numerical method seeking an approximated solution of the distribution of field variables in the problem domain that is difficult to obtain analytically. It is done by dividing the problem domain into several elements and applying, afterwards, known physical laws to each individual element (that usually have a simple geometry). The elements are formed by nodes whose piecewise linear functions approximate a continuous function of an unknown field. The unknowns are then the discrete values of the field variable at the nodes. Afterwards, the equations for the elements are established using proper principles, "tying" the elements to one another. This process leads to a set of linear algebraic simultaneous equations for the entire system that can be solved to yield the required field variable. [24]

This process is closely tied to the Computer Assisted Design since, as seen in figure 2.14, after testing, if the results are not optimal, the product returns to the drawing board and the process repeats itself until the requirements of the product are met.

With these new project tools, it is also possible to make the structural analysis and the design simultaneously. Which is something that makes the process much quicker and more cost effective.

2.6 Summary

The motorcycle industry has evolved throughout history. Since the beginning there were numerous inventions that made the motorcycle what it is today.

Nowadays motorcycles are more reliable and safe and there are various types to satisfy the different customers and purposes.

The types of chassis previously shown translate the large amount of designs that are possible. Although, it is necessary to add that these are not all of them, and more than often, there are frame designs that comprise more than one of these ideas. All of them confer advantages and limitations and it is up to the constructors to use what suits them the most and to decide which of them (or which combination of them) is more advantageous for their motorcycle.

Also, the manufacturing process has evolved throughout the years having now a big part of the development based on computational methods such as CAD and the FEM.

Chapter 3

The Frame

An analysis can only be properly made if the part (or parts) studied are adequately understood. For that matter, this chapter contains an explanation of the design choices as well as a simple description of the materials used on the various parts.

The chassis developed by AJP Motos is comprised of multiple parts and is a combination of the past experience of the company in the motorcycle manufacturing market.

With this frame, AJP Motos, is trying to enter the trail motorcycle segment. The main characteristics sought in this frame are the low weight and good handling. To achieve this, aluminium was employed as a material, while keeping the use of steel to reduce the price of the vehicle. The performance of this new motorcycle off-road is also a major concern of this company, whose motorcycles are created mainly for recreational Enduro use.

3.1 Steel Parts

Steel is easy to work with and easy to weld. It is also easy to machine and deform. All the components to be produced in this material will be grouped in one single subsection as all of them will form a single part.

The steel used in this construction was the E195/S3 (EN 10305-3) and its properties are explicit in the Table 3.1.

Table 3.1: Properties of the steel to be used on the chassis

Material	**Designation**	σ_y	σ_u	E	ρ
Steel	E195/S3 (EN 10305-3)	250	330	200	7850
		MPa	MPa	GPa	Kg/m^3

The steel is to be employed on the parts that need to be welded as it makes the process less difficult (aluminium is not as easy to weld) and, consequently, cheaper.

3.1.1 Oil Tank, Steering Column and Engine Cradle

Figure 3.1: Oil Tank, Steering Column and Engine Cradle

Unlike most motorbikes, the oil tank to be implemented on this new model is inside the frame. This is possible by making the part between the steering column and the backbone hollow. However, with this design it is necessary to pay extra attention when creating the concept and building the part, since no leaks should be verified during the use of the machine. The oil tank is composed of two parts made by metal forming that are welded together. While being made of thin metal, the part still needs enough stiffness to withstand bending, lateral and torsional loads.

The steering column is a simple tube that is welded to the oil tank, there the fork and front suspension will be coupled with the rest of the chassis.

To connect the engine cradle, a hollow square beam is used. This confers the chassis enough bending and torsional stiffness while keeping it with low weight. Having this part

and a cradle also creates more protection for the engine, since, when off-road, the clash of the engine with the ground is a possibility. Even so a protective plate should be placed.

The lower cradle is comprised of two bent tubes that link the hollow beam previously mentioned to the back of the cradle and a tube that connects both of these creating a closed loop. The tube in the back is to be connected to the lateral beams (Subsection 3.2.2) where the feet supports will be placed.

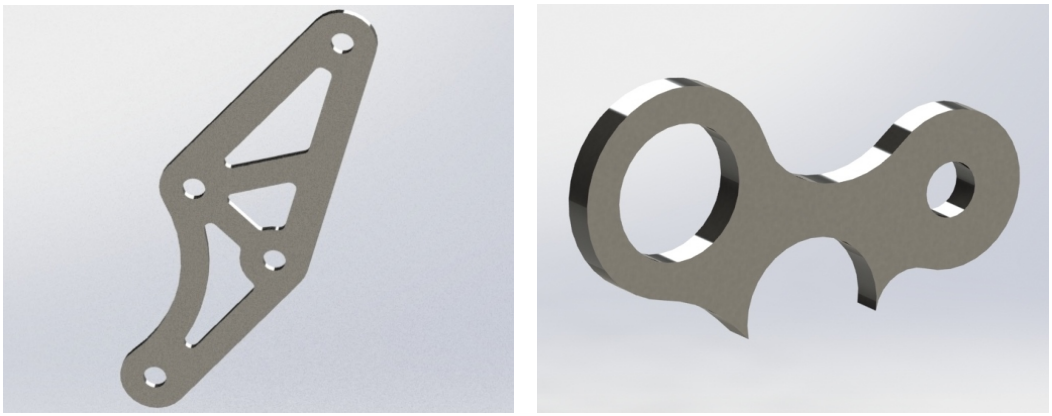

(a) Engine Support Plate (b) Connecting Rod Support

Figure 3.2: Engine Connection Parts to the Cradle

The engine will be connected to this part on the front and on the rear. On the front it will be connected with the aid of two metal plates as shown in the Figure 3.2(a) and on the rear through the supports of the connecting rod as shown in Figure 3.2(b). The frontal support is to be connected using bolts and the supports in the rear will be welded to the tube in the back of the cradle.

All the parts cited in this subsection will be made of steel, since some will be made through metal forming and the majority them will be welded to each other. This makes the welding process much easier and cheaper as referred in the beginning of this chapter.

3.2 Aluminium Alloy Parts

The aluminium alloy will be used in parts that are easier to make through casting. Employing this alloy also allows the motorcycle to be lighter as the aluminium density is much lower than the steel's, as it can be seen in Table 3.1

A good economy of scale is also sought, as the same aluminium alloy will be used in various parts and even in other models of the brand.

Table 3.2: Properties of aluminium alloy to be used on the chassis

Material	**Designation**	σ_y	σ_u	E	ρ
Cast Aluminium	AlSi7Mg0,3 (Calypso® 67B)	165	270	70	2770
		MPa	*MPa*	*GPa*	Kg/m^3

The parts to be made using cast aluminium are highlighted in the Figure 3.3. It is possible to see that most of the back of the chassis will be created through this procedure.

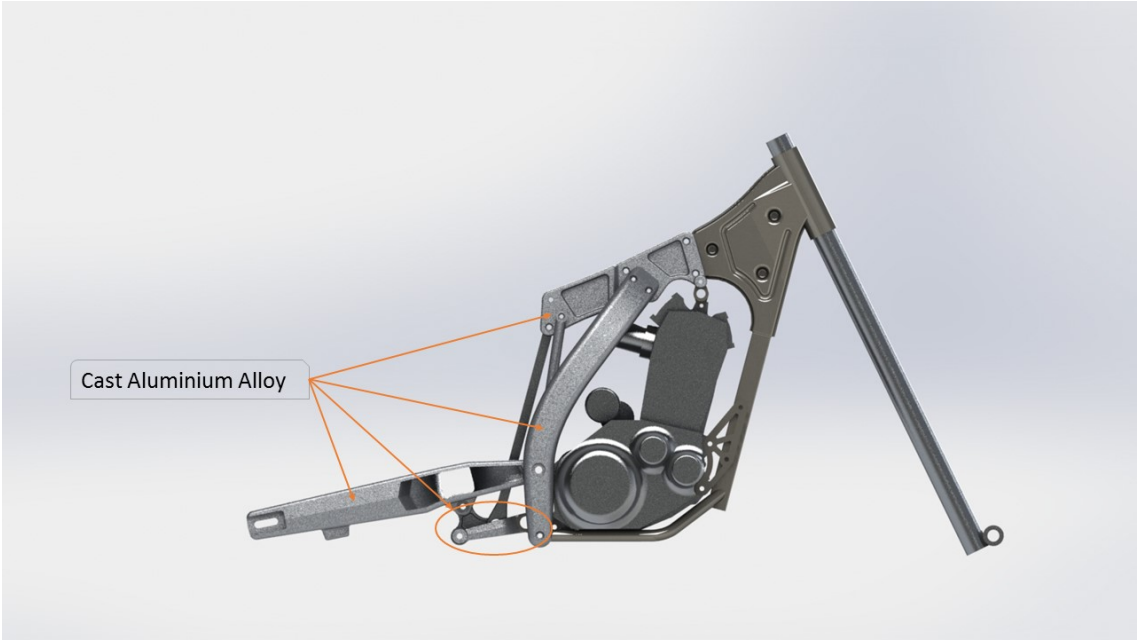

Figure 3.3: Cast Aluminium Alloy parts in the full model

3.2.1 Backbone

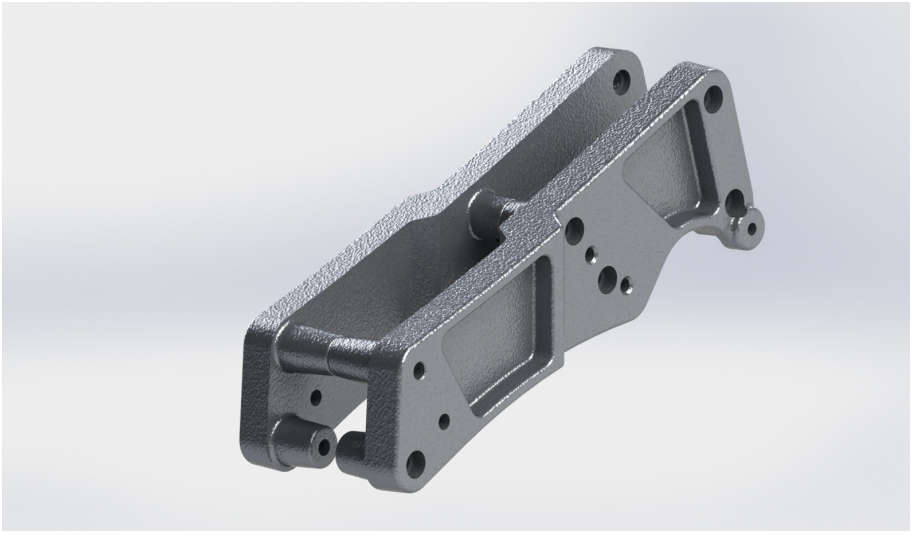

Figure 3.4: Chassis Backbone

Being the main part of the motorbike it can be classified as the "Backbone", although it is not as the backbones previously mentioned.

It is composed by two parts, one for each side, that are joined during the assembly with the use of bolts.

This part connects to the oil tank (inside the front part of the chassis, as shown in the Subsection 3.1.1) through the help of four bolts and two small plates welded to the oil tank, as shown in Figure 3.5. On both sides there is a side beam attached and on the rear two rods on each side. These rods add bending stiffness to the frame and help keeping the shock absorber centred. This one is placed on the very rear in the middle of both backbone side parts.

There is also an engine support in this part, that, in conjuncture with the supports on other parts, will make the engine a structural part of the chassis and add extra stiffness to the structure as referred in the section 2.2.7.

The purpose of this part is to keep everything connected and add enough bending and lateral stiffness to keep the rider safe and comfortable as well as sustaining all the forces transmitted through the damper to the main frame.

The use of aluminium makes this part lighter than a part made for the same purpose built in steel.

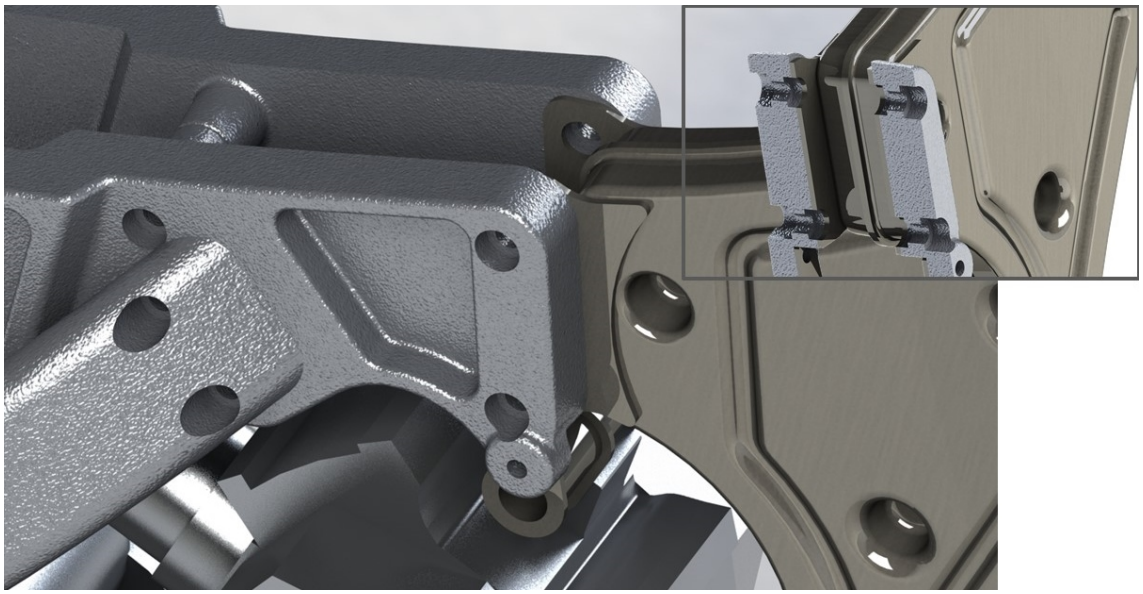

Figure 3.5: Connection detail of the Backbone to the Oil Tank

3.2.2 Lateral Beams

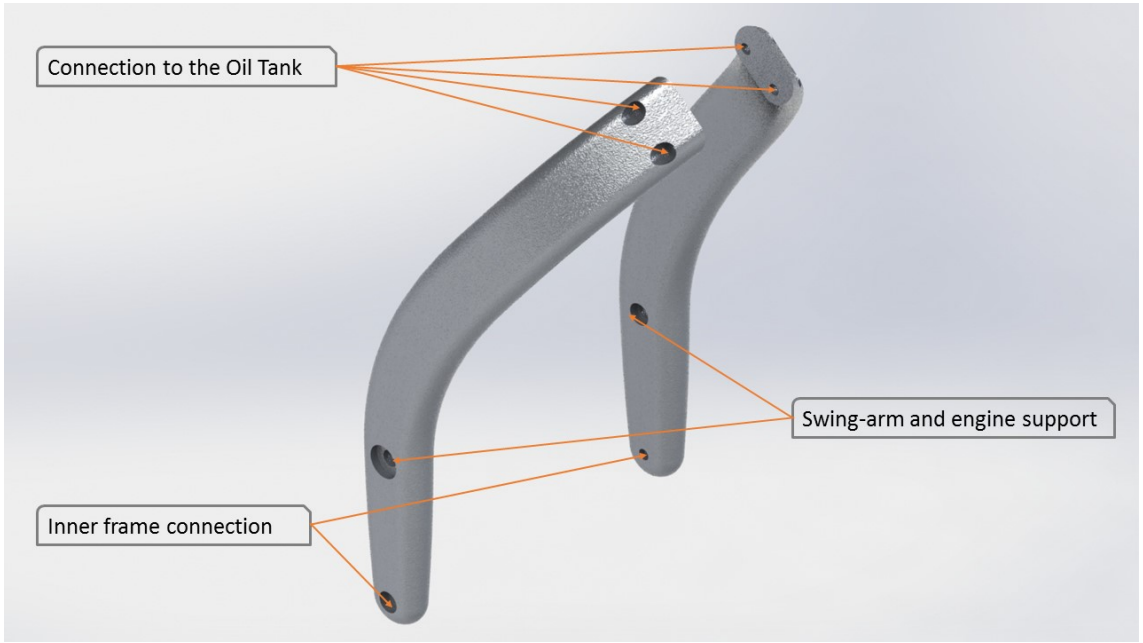

Figure 3.6: Left and right side Beams

These side beams are cast from the aluminium alloy referred before on the Table 3.2. They add torsional and bending stiffness to the chassis and connect the backbone to the swing-arm.

The beams are hollow, as shown in Figure 3.7, to decrease the weight of the structure.

Figure 3.7: Lateral Beam inside detail

Structurally they need to keep the cradle and the backbone connected and without relative movement. Also, as the connection to the swing-arm, it is needed that these parts withstand the stress and fatigue transmitted from the rear wheel (through the swing-arm) to the main chassis.

3.2.3 Swing-arm

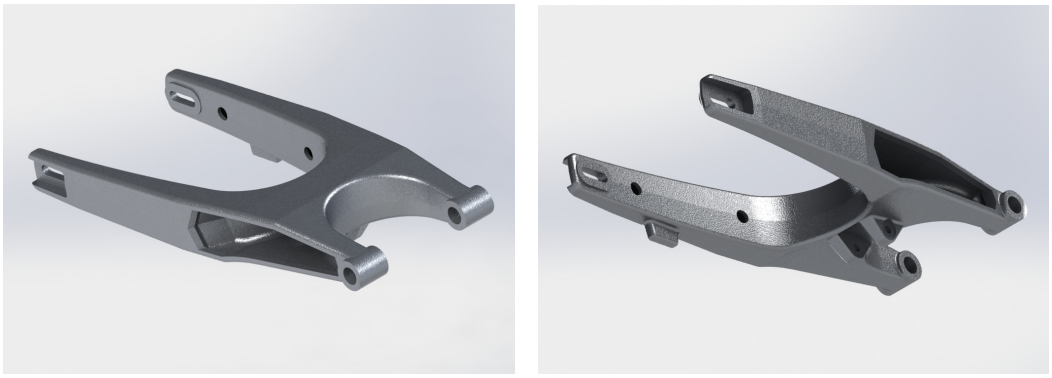

(a) Top (b) Bottom

Figure 3.8: Swingarm

The swing-arm is the structure where the rear wheel is mounted. It has to be able to deal with the stress caused by the rear wheel in all situations (jumping, cornering, accelerating, etc.).

As it was proven in earlier models of AJP Motos, making the swing-arm in cast aluminium is a good choice. Therefore, this one will follow the same procedure. The part is completely hollow with an almost constant wall thickness (Figure 3.9), so it makes the casting easier as well as reducing the weight.

Figure 3.9: Swing-arm inside detail

3.2.4 Connecting Rods

The connecting rods will be made of cast aluminium as the geometry is much easier to achieve through this method. The same alloy will be employed for the reason mentioned in the beginning of this chapter.

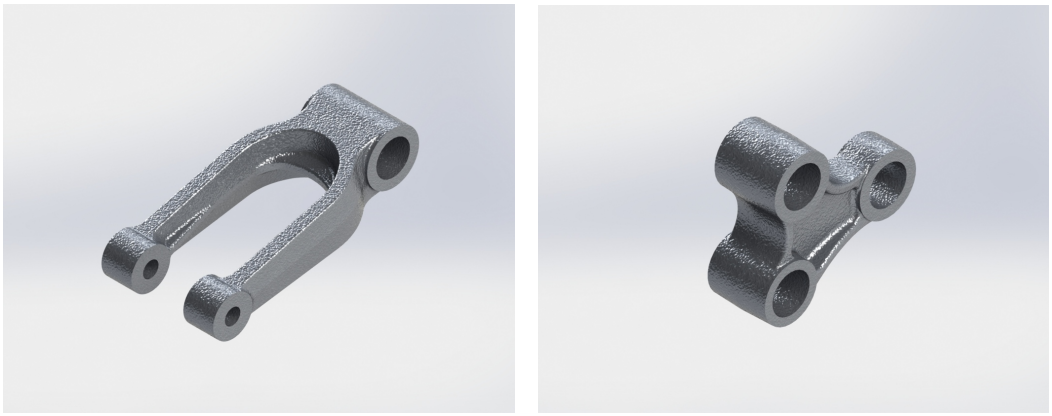

(a) Chassis Connecting Rod (b) Swing-arm Connecting Rod

Figure 3.10: Connecting Rods

3.3 Other Parts

The full assembled chassis contains more parts than what is described, but for this analysis they will be considered as rigid. The fork is already tested and thus does not need further testing. As for the rear shock absorber, it will be also considered rigid, as its specifications are not known, making the analysis containing this one considered extreme (the stresses will not be as high as the analysis implies).

3.4 The Engine

The engine to be used in this motorcycle is the same as the one used on the Yamaha XTZ 660. In this analysis it will be considered rigid as it is a strctural part of the chassis. The engine specifications are shown in Table 3.3.

It should be noted that this is the biggest engine to be employed in an AJP Motos model. The bigger engine is expected to give the riders the opportunity to travel with this motorcycle in the open road and even highways.

Table 3.3: Engine Specifications [26]

Engine Type	Single Cylinder
Displacement	660 cc
Bore x Stroke	100.0 mm x 84.0 mm
Compression Ratio	10.0 : 1
Maximum Power	35.0 kW (46.9 hp) @ 6000 rpm
Maximum Torque	58.0 Nm @ 5500 rpm
Lubrication System	Dry Sump
Clutch Type	Wet, Multiple-disc Coil Spring
Carburettor	Electronic Fuel Injection
Ignition System	TCI
Starter System	Electric
Transmission System	Constant Mesh, 5 Speed
Final Transmission	Chain
Weight	51 kg (Oil Included)

3.5 Summary

As all the frames, this one is comprised of multiple parts. These parts, in this case, are made of two different materials: an aluminium alloy and a steel (Table 3.4).

Each part has it's function and the frame needs all of them working as one to fulfil the role it has on the motorcycle.

In this case the engine is also a structural member of the motorcycle, so it is also a part of the chassis.

The full frame dictates the shape of the motorcycle and contains the performance features of the same.

Table 3.4: Properties of the materials to be used on the chassis

Material	**Designation**	σ_y	σ_u	E	ρ
Cast Aluminium	AlSi7Mg0,3 (Calypso® 67B)	165	270	70	2770
Steel	E195/S3 (EN 10305-3)	250	330	200	7850
		MPa	MPa	GPa	Kg/m^3

Chapter 4

Structural Analysis

The analysis should cover all the possible solicitations the chassis may encounter through it's life. Therefore, for a complete analysis, multiple case studies where conceived.

As a first step a pre-study was made using the geometry given by AJP Motos using the *Solidworks*® software. The values obtained with this method were not accurate since discontinuities were found in the displacements (Appendix A).

After this procedure it was decided that the best approach would be to use the software *ANSYS*® *Workbench 15.0*. This would lead to a simpler interface to create the different studies.

To obtain faster solving times and to lower the number of parts, the model was simplified. All the parts that were to be welded were joined in a single part, as shown in the Figure 3.1. The engine mounts in the front were also joined, along with the bushing, to the structure mentioned before. The rear shock absorber support rods were coupled to the backbone and remade for a better fit. The engine support that connects the backbone to the engine was also put in a single part due to several errors that appeared when they were separated (the various parts of this support would expand inexplicably).

The load applied was devised considering the total motorcycle weight to be the same as this model's market opponents (around 200 kg) and a rider with 100 kg. The 100 kg for the rider my be considered too much, but more than often, the riders carry extra load on their motorcycle. Applying a security coefficient of 3 and approximating the gravitational acceleration 10 m/s^2, a force with 9000 N was calculated.

Due to the lack of standardized loads to be applied in the study, the results can only be analysed without any guarantees until an experimental test is done. For this reason, a series of tests were also devised in addition to the cases recreating the various situations extracted from the normal usage of an off-road motorcycle. This was based on the Table 4.1 specified by Vittore Cossalter in his "Motorcycle Dynamics" book. For this test a

load of 1 kN or a moment of 1 kNm was applied according to the different cases.

Table 4.1: Stiffness Values for Each Component [27]

Component	**Torsional** ($kNm/^{o}$)	**Lateral** (kN/mm)	**Vertical** (kN/mm)
Main Frame	3-7	1-3	5-10
Swing-arm	1-2	0,8-0,16	n/a
Fork	0,1-0,3	0,07-0,018	n/a

The stiffness can be calculated dividing the load applied for the displacement (Equation 4.1) or in the case of a moment, divided by the rotation (Equation 4.2).

$$k = \frac{F}{\delta} \tag{4.1}$$

$$k = \frac{M}{\theta} \tag{4.2}$$

4.1 Mesh

The mesh used in this analysis was made by the tetrahedrons method using a patch conformed algorithm included in *ANSYS® Workbench 15.0*.

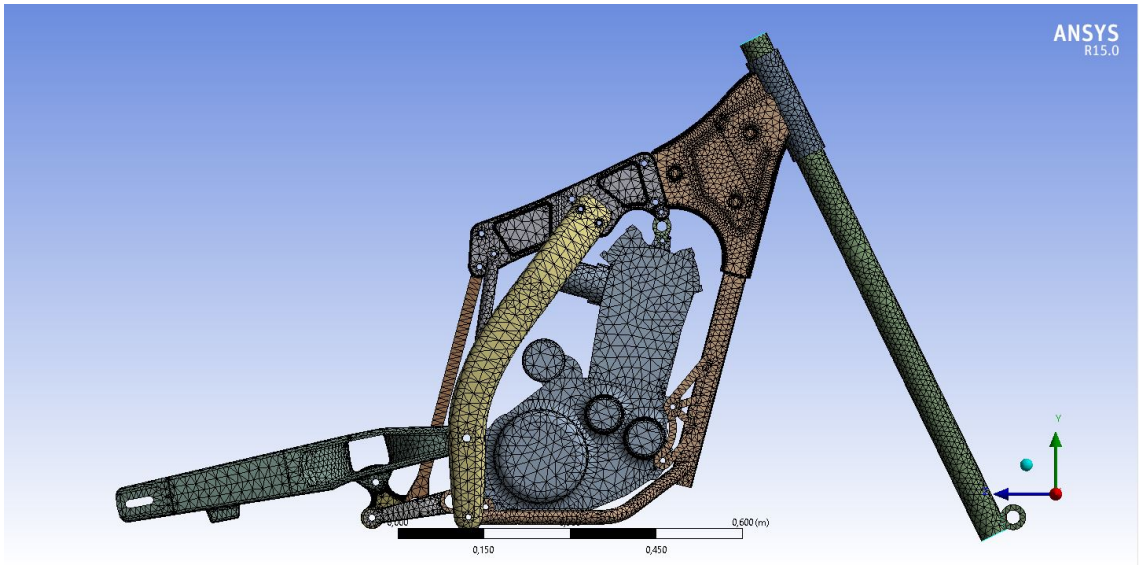

Figure 4.1: Mesh used in the analysis, generated by *ANSYS® Workbench 15.0*

It is possible to see that the oil tank presents smaller mesh elements as it is a critical spot for the chassis, as referred in the subsection 3.1.1.

This mesh provided good results and the running time for each case did not take a long time. It has 171.671 tetrahedral elements and 318.221 nodes.

Some convergence tests were done to validate the mesh and it was possible to conclude that this mesh, with the number of elements mentioned before, presents a good approximation for the model.

4.2 Case 1: Landing with both wheels

4.2.1 Analysis Parameters

For the first set-up, the whole model was analysed. The idea behind this case was to simulate the stresses that the frame suffers when the landing of a jump is done with both wheels. The landing of a jump was chosen because it takes to the extreme the forces applied during a normal ride or simply standing still (vertically).

To simulate the landing, the ends of the fork and swinging arm were constrained to simulate the wheels. On the fork it was used a cylindrical support with the tangential movement not restrained, to allow rotation but not displacement on the direction of any axis. For the swing-arm, the lateral and vertical movement were constrained, but the displacement along the longitudinal axis was left free (along Z axis in Figure 4.2).

In this case the forces were applied in the feet supports, as, when landing, the riders tend to stand on them.

Exceptionally for this case, two different orientation vectors were devised and tested, one being vertical, Figure 4.2(a), and another oriented downward and backward (to simulate the direction of the legs of the rider), Figure 4.2(b). The loads and supports are thoroughly presented in the Table 4.2

To simplify the calculations, the totality of the load was applied on the supports, as it is known that this is not the case verified in reality. Also, the motorcycle weight can be applied in the center of mass which is around that area, only a little bit up.

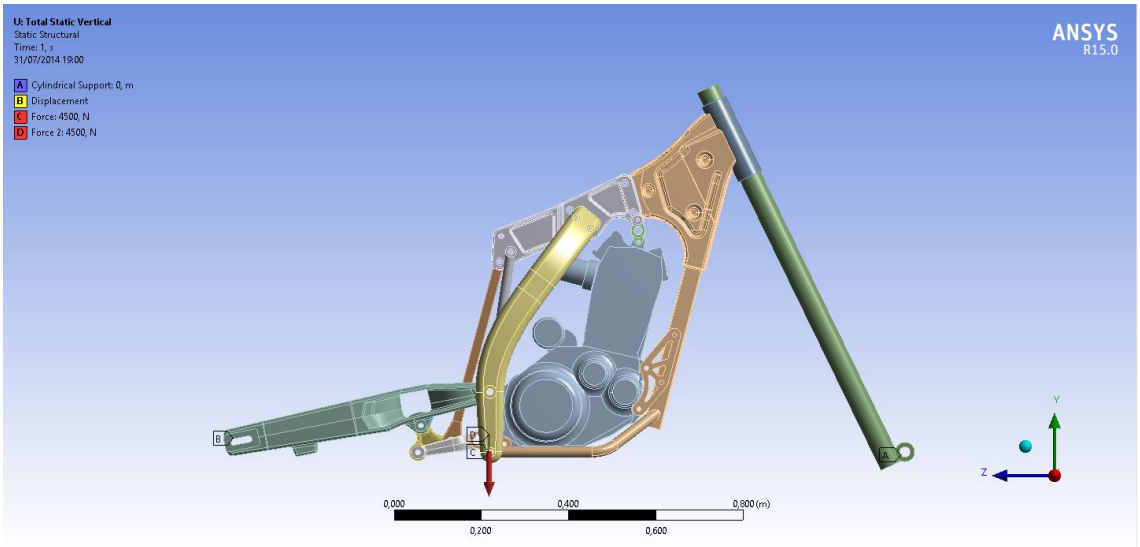

(a) Vertical Load

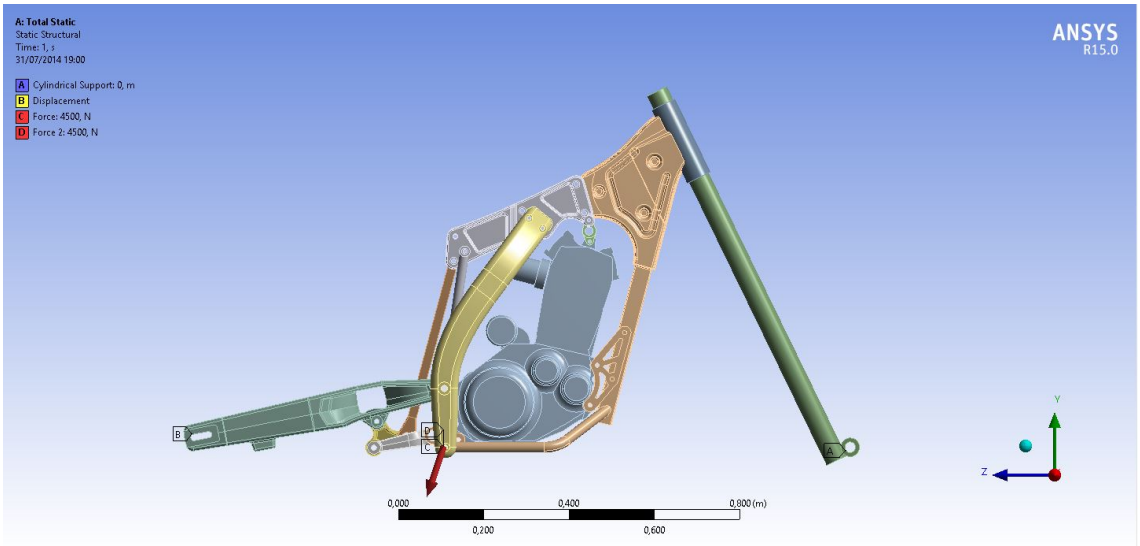

(b) Rider aligned Load

Figure 4.2: Case 1 parameters introduced in *ANSYS® Workbench 15.0*

Table 4.2: Loads and Supports applied in Case 1

Load Case	Type	Figure Tag	X	Y	Z	RX
Vertical	Support	**A**	Fixed	Fixed	Fixed	Free
	Support	**B**	Fixed	Fixed	Free	Free
Figure 4.2(a)	Load	**C**	0 N	-4500 N	0 N	–
	Load	**D**	0 N	-4500 N	0 N	–
Rider Aligned	Support	**A**	Fixed	Fixed	Fixed	Free
	Support	**B**	Fixed	Fixed	Free	Free
Figure 4.2(b)	Load	**C**	0 N	-4269,07 N	1423,02 N	–
	Load	**D**	0 N	-4269,07 N	1423,02 N	–

4.2.2 Results

When landing with both wheels the loads are well distributed, so the stresses are quite evenly shared by the front and rear of the chassis.

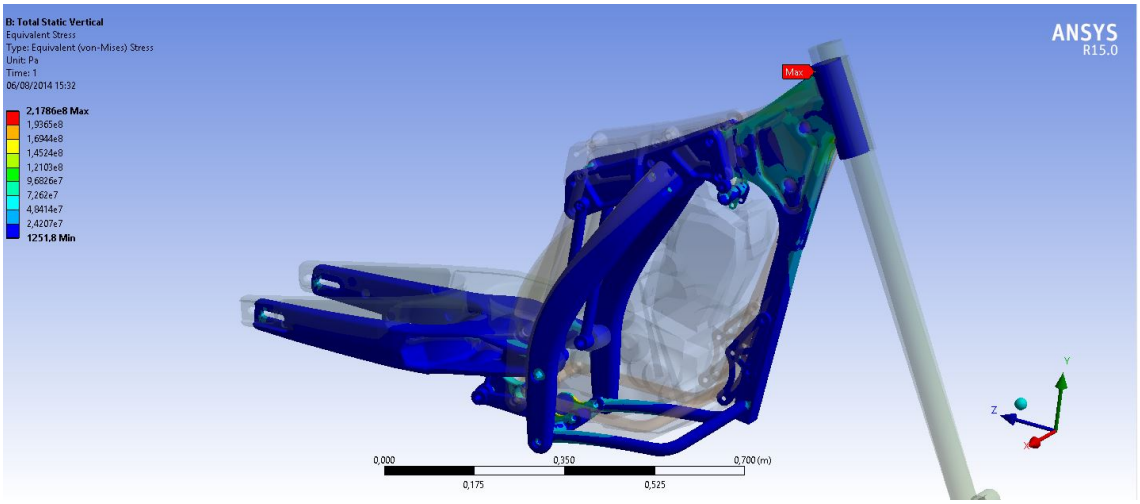

(a) Vertical Load

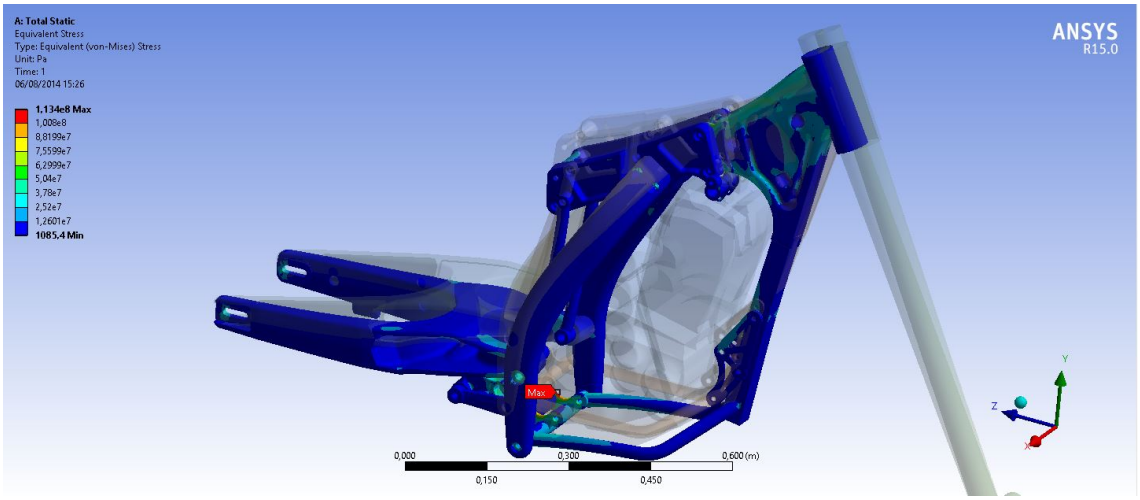

(b) Rider aligned Load

Figure 4.3: Case 1 results extracted from *ANSYS® Workbench 15.0*

Even with similar loads, it is possible to see that both have different maximum stress points and values.

The vertical load presents a higher stress near the steering column, as seen in Figure 4.3(a). The value (217,9 MPa), however, is still lower than the steel's yield strength shown in the Table 3.4. On the aluminium parts, the maximum stress was registered on the left side lateral beam with a magnitude of 87,2 MPa, also below the aluminium yield strength.

When subjected to the rider aligned load, the maximum stress was located on the left connecting rod support with a value of 113,4 MPa, a value much lower than the one mentioned before. As before, the highest stress registered on the aluminium parts was on the left lateral beam, this time with 63,5 MPa.

As it is, it can be seen that the chassis has a slight disequilibrium to the left side. Also, it is noticeable that with this kind of loads, the critical points are located in the connecting rod supports and on the area connecting the steering column to the oil tank. That said, even with a load three times the expected weight, the chassis used, on the worst situation, around 87% of it capabilities on the steel parts and 53% on the aluminium parts. In addition, the value of the maximum stress on the connecting area of the oil tank and steering column may also be exaggerated since the edges are too angular as welding will round the connection.

4.3 Case 2: Braking/Frontal Impact

The second case was based on the braking load applied to the frame (Figure 4.4(a)). However, while conceiving it, an idea was brewed just to watch how the chassis would fare against a frontal impact (Figure 4.4(b)).

In this case, when braking, it is considered that all the weight is supported by the front wheel, as it is supposed that when in maximum braking, the force on the rear wheel is null. [28]

4.3.1 Analysis Parameters

The load chosen to excite the frame was again the 9000 N, value that is well over the forces usually felt when braking. This time the load was applied on the end of the fork, place where usually the wheel is bolted on (Figure 4.4). Due to this, the constraints (supports) had to be changed. The longitudinal movement restriction was changed from the front wheel mount to the mount in the swing-arm, leaving the longitudinal movement free in the front wheel (Table 4.3).

The second sub-case, the frontal impact, may be not as useful as the braking one, however, as we are studying the frame, more information translates in more situations covered.

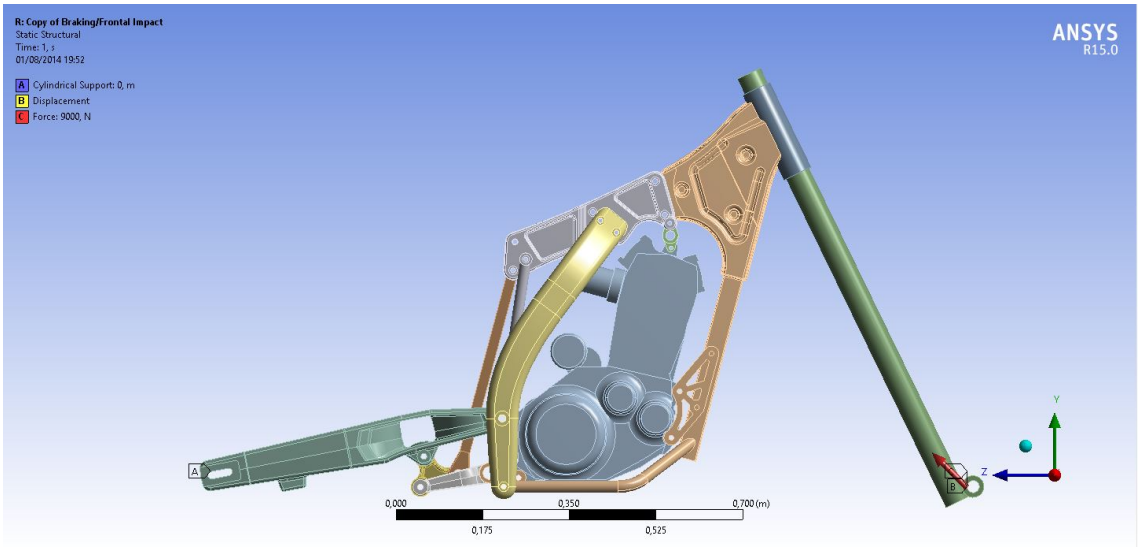

(a) Braking

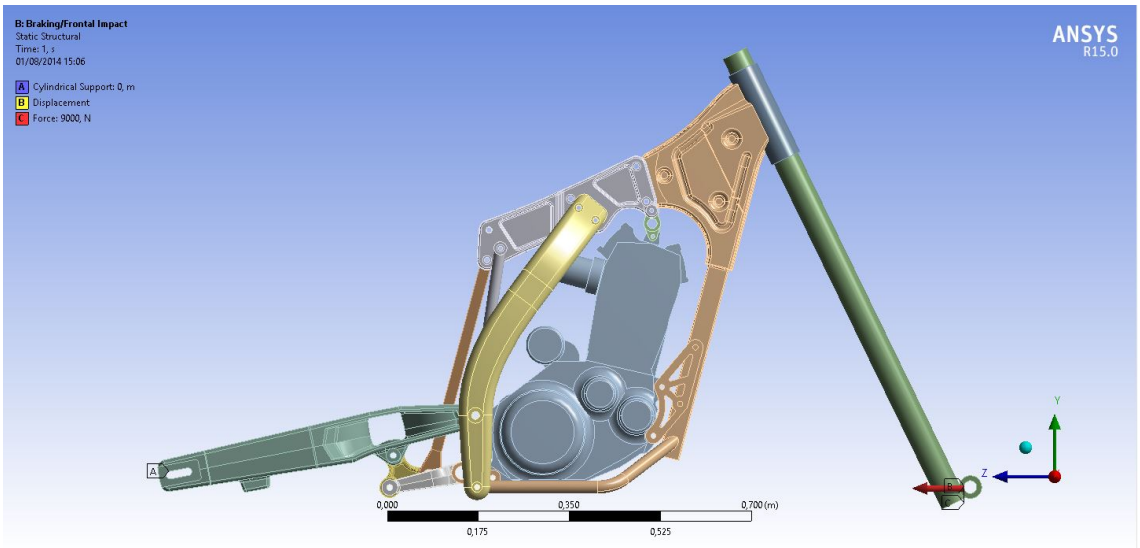

(b) Frontal Impact

Figure 4.4: Case 2 parameters introduced in *ANSYS® Workbench 15.0*

Table 4.3: Loads and Supports applied in Case 2

Load Case	Type	Figure Tag	X	Y	Z	RX
Braking	Support	**A**	Fixed	Fixed	Fixed	Free
	Support	**B**	Fixed	Fixed	Free	Free
Figure 4.4(a)	Load	**C**	0 N	6363,96 N	6363,96 N	–
Frontal Impact	Support	**A**	Fixed	Fixed	Fixed	Free
	Support	**B**	Fixed	Fixed	Free	Free
Figure 4.4(b)	Load	**C**	0 N	0 N	9000 N	–

4.3.2 Results

The results are similar, however, in the braking case the force applied has a vertical component as well as a horizontal component when the frontal impact only presents an horizontal component. This causes the frame to have mainly displacements in the horizontal direction on the latter case and a combination of both horizontal and vertical displacements on the first case.

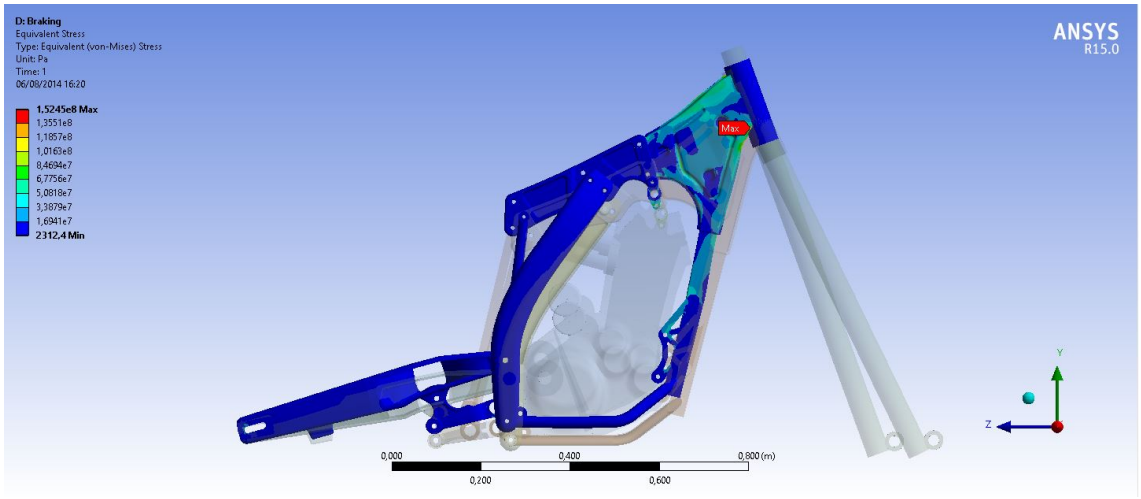

(a) Braking

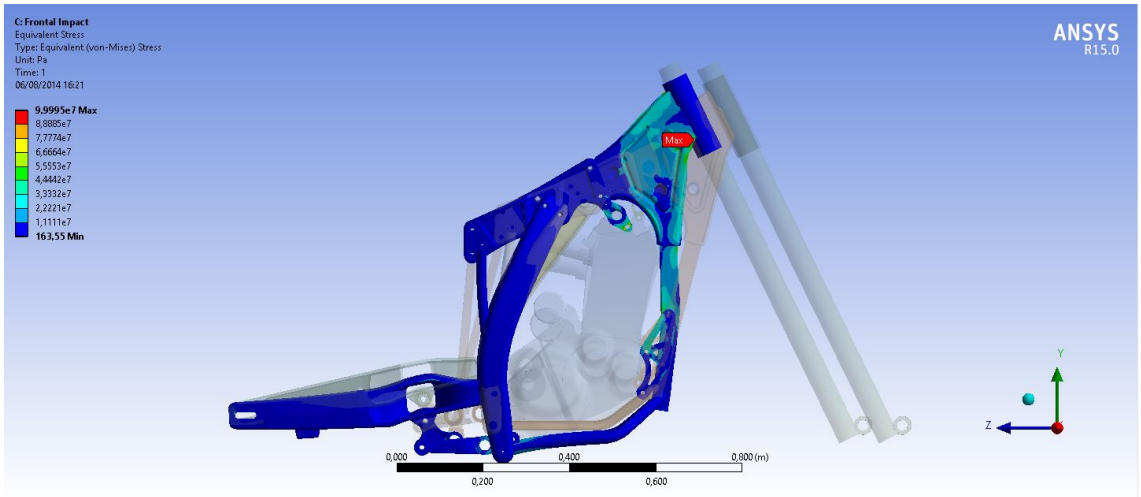

(b) Frontal Impact

Figure 4.5: Case 2 results extracted from *ANSYS® Workbench 15.0*

This said, as expected, the case with higher stresses was the braking case. However, the maximum stresses verified were on the oil tank connection to the steering column on both cases having a value of 152,4 MPa on the braking case and 100 MPa on the frontal impact case.

Compared to the steel parts, the stresses obtained on the aluminium parts are much lower, being only around 30 MPa.

As well as the values obtained on the study 4.2, these are lower than the maximum yield strength of both materials. Also, as said before, these values may be exaggerated due to the final geometry of the connection not being as angular as the one studied. The disequilibrium observed before is not as evident here but it still happens near the backbone area so it is most likely caused by the engine connection to the frame.

4.4 Case 3: Landing on the back wheel

4.4.1 Analysis Parameters

After a jump, motorcycles usually do not land with both wheels at the same time, so, to maximize the load, it was considered that the motorcycle landed in the back wheel only.

To simulate this, the frame was restrained on the feet supports, to follow the same principle mentioned before. The load was then applied on the swing-arm with a value of 9000 N, as before.

As the impact occurs initially on the swing-arm, it was decided to isolate it and test under the load mentioned before, but this time applying a cylindrical support on the swing-arm fixtures and a displacement restrain in the Y axis on the rod connection (Figure 4.6(b). This last approach was done so that it would be possible to compare with a previous work for AJP Motos [6].

Table 4.4: Loads and Supports applied in Case 3

Load Case	Type	Figure Tag	X	Y	Z	RX
Whole	Support	**A**	Fixed	Fixed	Fixed	Fixed
	Load	**B**	0 N	4500 N	0 N	–
Figure 4.6(a)	Load	**C**	0 N	4500 N	0 N	–
Swing-arm	Support	**C**	Fixed	Fixed	Fixed	Free
	Support	**D**	Free	Fixed	Free	Free
Figure 4.6(b)	Load	**A**	0 N	4500 N	0 N	–
	Load	**B**	0 N	4500 N	0 N	–

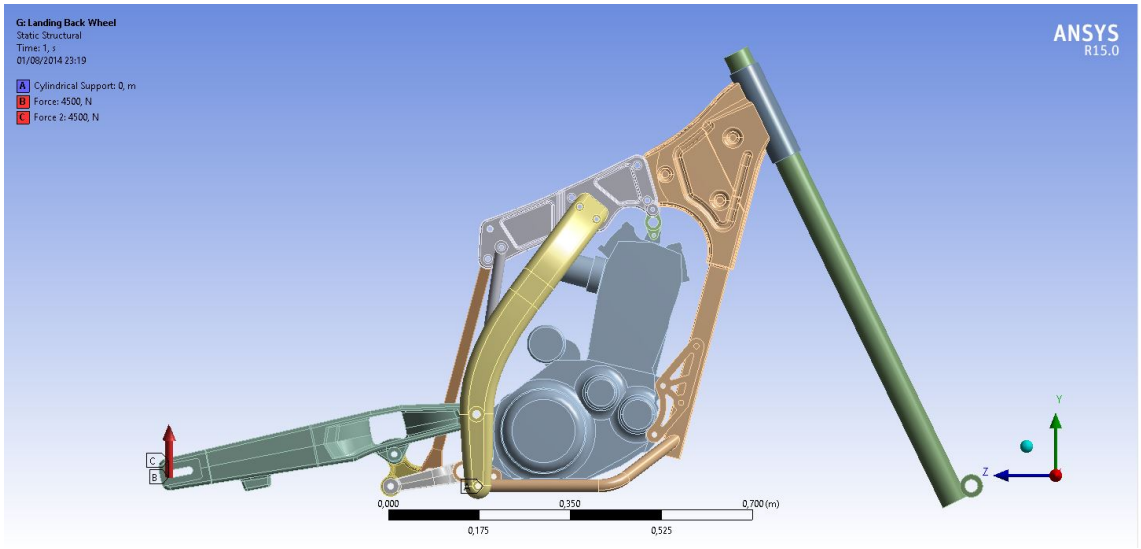

(a) Whole Structure

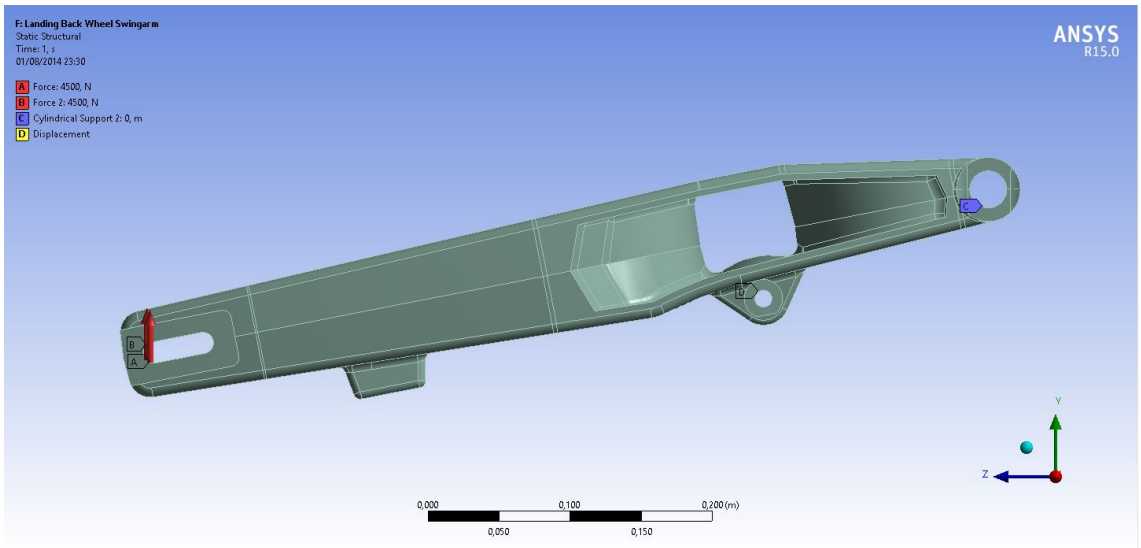

(b) Swing-arm Only

Figure 4.6: Case 3 parameters introduced in *ANSYS® Workbench 15.0*

4.4.2 Results

This case results present a maximum stress much higher than the yield strength or the ultimate tensile strength of the steel used. A stress of 819,6 MPa on a steel part means it would break instantly if subjected to this force. Additionally, the forces applied were three times higher than the weight of the motorcycle and the maximum stress read is more than three times the value of the maximum yield strength. It means that if the whole motorcycle plus the rider landed only in the back wheel, the part would suffer from

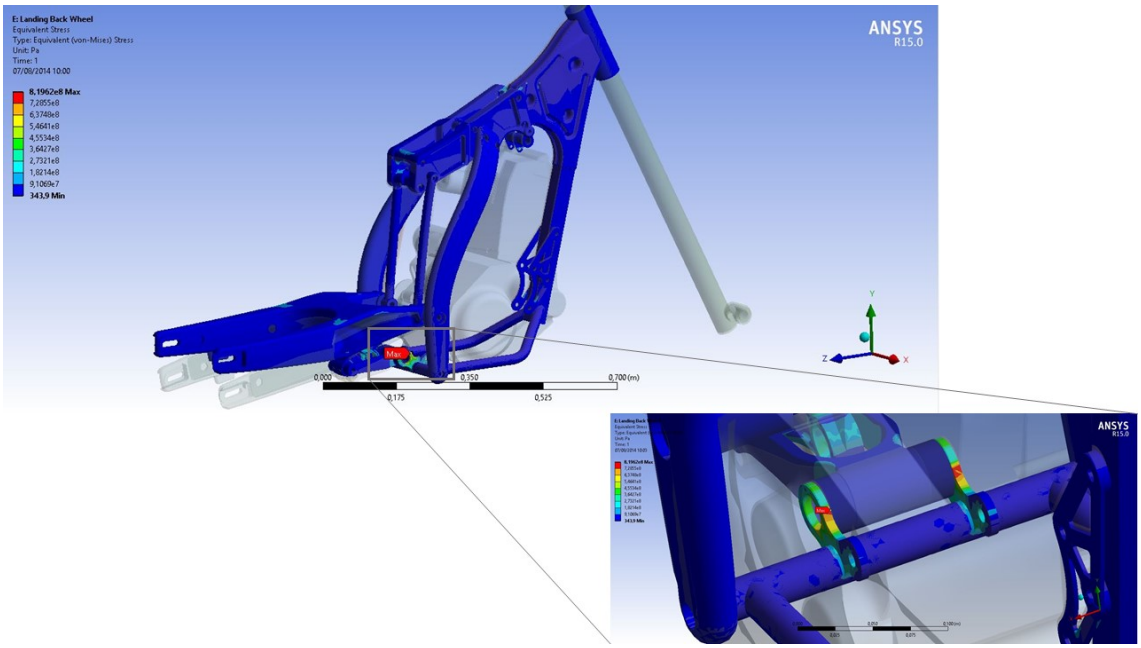

Figure 4.7: Case 3 results extracted from *ANSYS® Workbench 15.0* for the whole structure

irreversible deformation. For this reason, an optimization of the design had to be thought of (Subsection 4.4.3).

Stresses higher than both the maximum yield strength and the ultimate tensile strength on the connecting rods were also registered (387,5 MPa was the maximum stress in these parts). This is something that should be addressed and looked at since the shock absorber was considered rigid and may be the only cause of this high stresses.

As for the swing-arm, the stresses obtained through the whole structure analysis and the one made only with the swing-arm have different maximum values, as shown in figure 4.8.

The maximum stresses are read in the same points in both cases, however, in the whole structure case the value is much higher than in the latter case. The value observed when testing the swing-arm isolated from the structure presents 155,8 MPa as the maximum stress, a value within the maximum stress of the aluminium alloy and close to the one registered in Miguel Oliveira's thesis [6]. On the other case a maximum stress of 222,4 MPa is obtained, a value 75 MPa higher than the one pointed before and also a value higher than the maximum yield strength of the aluminium alloy used. This discrepancy should be addressed in the future with a road test, to monitor the stresses in that area.

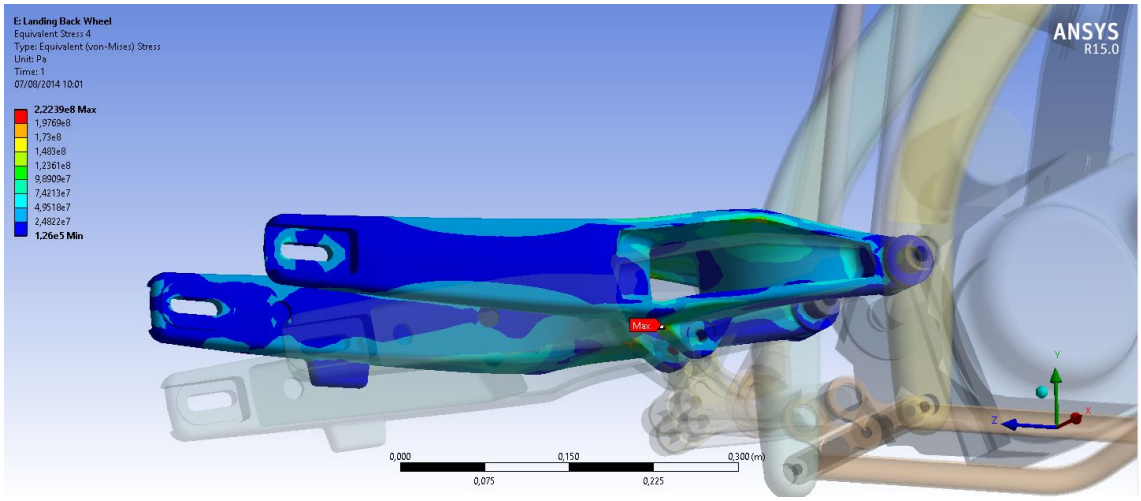

(a) Whole Structure

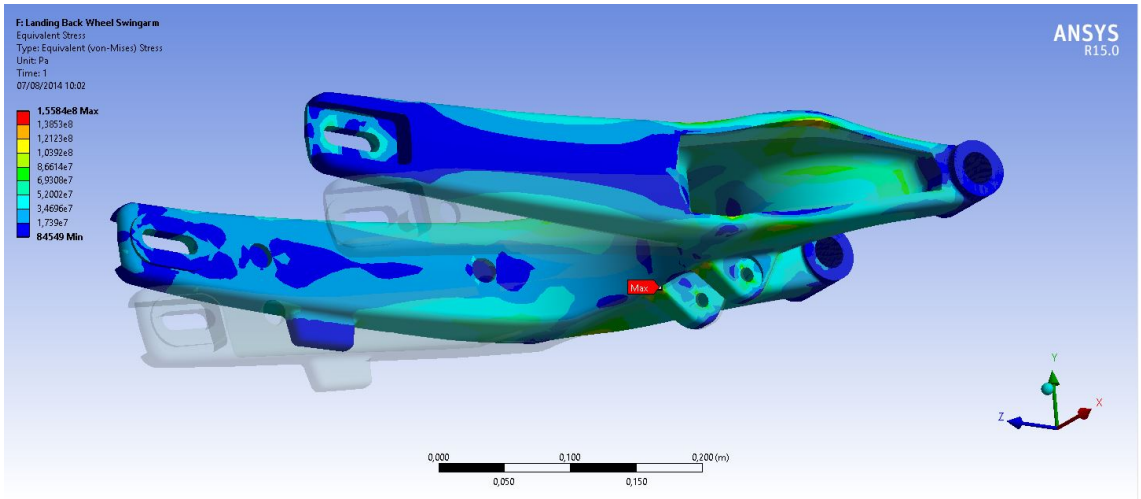

(b) Swing-arm only

Figure 4.8: Case 3 results for the swing-arm in the different approaches extracted from *ANSYS® Workbench 15.0*

4.4.3 Optimization

The starting point of this optimization was the thought of reducing the stress concentration factor in between the holes of the connection support.

If the shape of the connection rod support was less curvy, the accumulated stresses in between both holes would be lower (the stress concentration factor would be lower). With this in mind a new design was made with a straight line in between both holes instead of a curve and also with a straight line on the end to make the connection with the lower frame stronger.

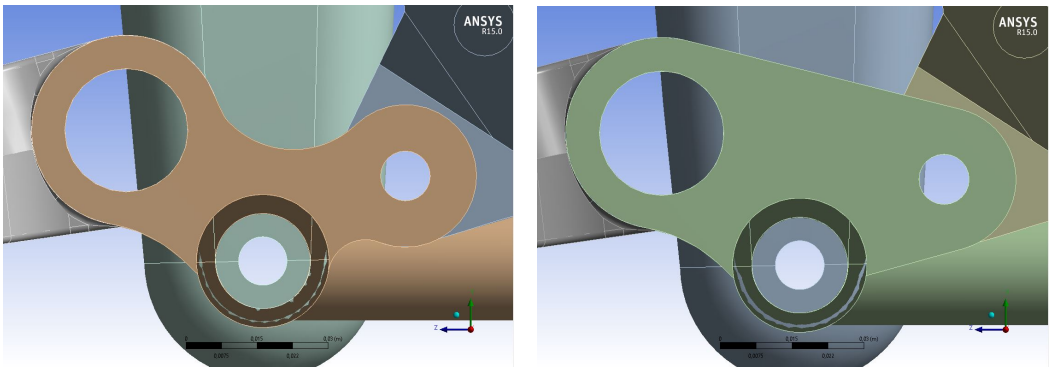

(a) Original design (b) Re-design

Figure 4.9: Original and re-designed connecting rod supports

This change in the design reduced the stresses in the connecting rods by half, as seen in the Figure 4.10

For a further reduction of the stresses, the width of the supports can be increased so that the area of the sections is also augmented, leading to the said result.

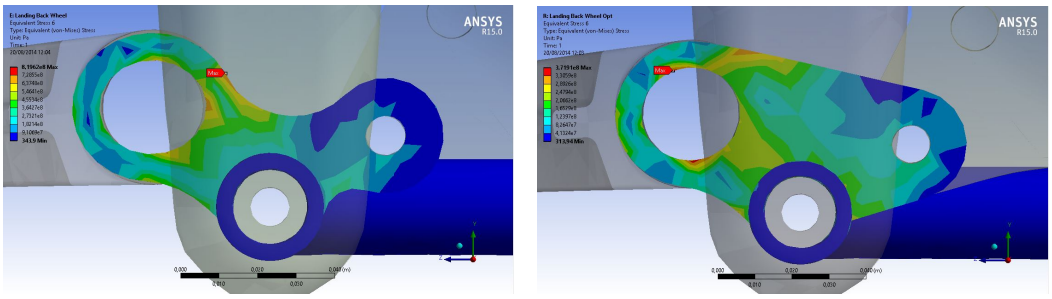

(a) Original design (b) Re-design

Figure 4.10: Comparison between the stresses with the original design and the re-designed connecting rod supports extracted from *ANSYS® Workbench 15.0*

Table 4.5: Comparison between the stress values of the original design and the re-designed connecting rod supports

	Original	**Re-designed**	**Reduction**
Maximum Stress	819,62	371,91	54,62 %
	MPa	*MPa*	–

4.5 Case 4: Landing only with the front wheel

4.5.1 Analysis Parameters

This may seem like an unimportant test as it may not happen regularly. The fact is that, as said before, the oil tank is a critical component for the motorcycle and in this design it is part of the chassis. So, to test thoroughly this area of the frame we have to devise loads that even if not usual, may happen.

To simulate this, a load was applied on the front wheel mount and, as before, the only restrain was on the feet supports , as seen in Table 4.6.

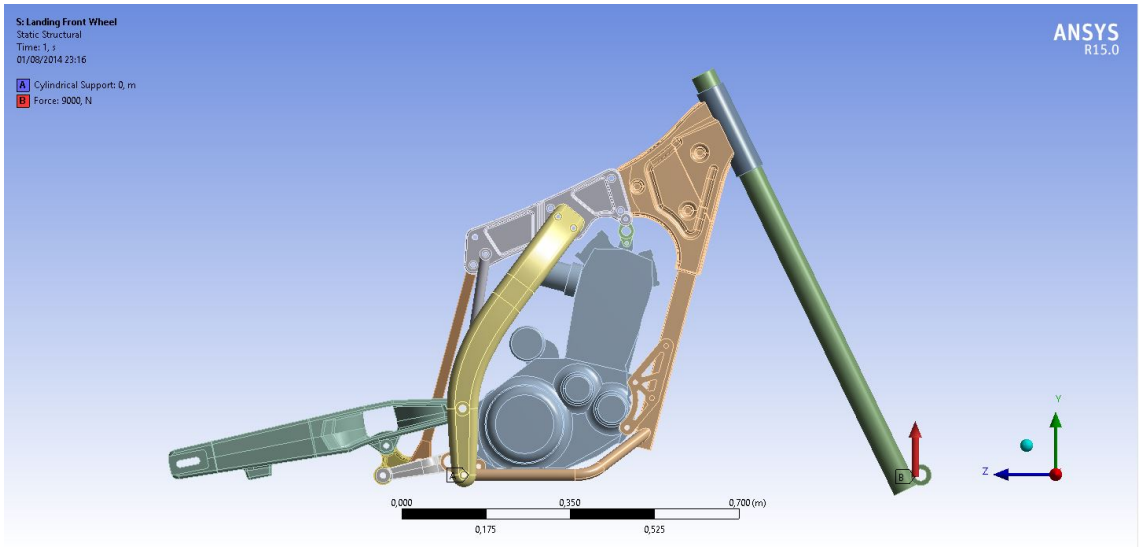

Figure 4.11: Case 4 parameters introduced in *ANSYS® Workbench 15.0*

Table 4.6: Loads and Supports applied in Case 4

Load Case	**Type**	**Figure Tag**	**X**	**Y**	**Z**	**RX**
Landing Front Wheel	Support	**A**	Fixed	Fixed	Fixed	Fixed
Figure 4.11	Load	**B**	0 N	9000 N	0 N	–

4.5.2 Results

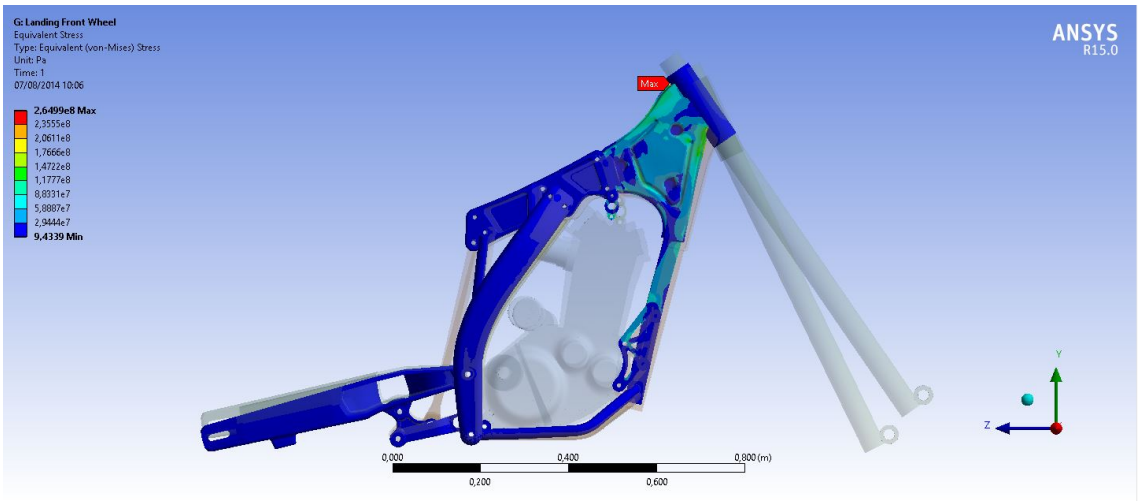

Figure 4.12: Case 4 results extracted from *ANSYS® Workbench 15.0*

The maximum stress on this part appeared, as expected, on the connection between the oil tank and the steering column. The value registered had a magnitude of 265 MPa and was placed on the edge of the "fin" of the oil tank. This value, however, decreases drastically in the vicinity, which indicates that it is highly influenced by the geometry. As it is, the part is still close to the maximum yield strength of the steel and, being this a situation that usually does not occur, it is still acceptable.

This, however, points to the importance of the attention needed for the weld in that point for the good functioning of the machine.

4.6 Case 5: Torsional Stiffness

The torsional stiffness is important for the good handling of the motorcycle. This test was devised so to provide a comparison between the torsional stiffness of this frame and the stiffness proposed by Vittore Cossalter (Table 4.1)[27].

Table 4.7: Torsional Stiffness Values extracted from Table 4.1

Component	**Torsional** ($kNm/^{o}$)
Main Frame	3-7
Swing-arm	1-2

4.6.1 Analysis Parameters

4.6.1.1 Main Frame

The first step was to devise a torsional analysis for the main frame. To that end, two cylindrical supports were applied to restrain the frame, one of them on the feet supports and another on the swing-arm connections to the frame, as shown in Figure 4.13. The moment applied was 1 kNm on the direction normal to the steering column. The moment was generated by two forces of 5 kN with opposed direction, as the distance between the middle of the column and each of the flat faces of the same is 10 cm. The forces are of the same magnitude and opposing directions to eliminate the lateral movement of the column.

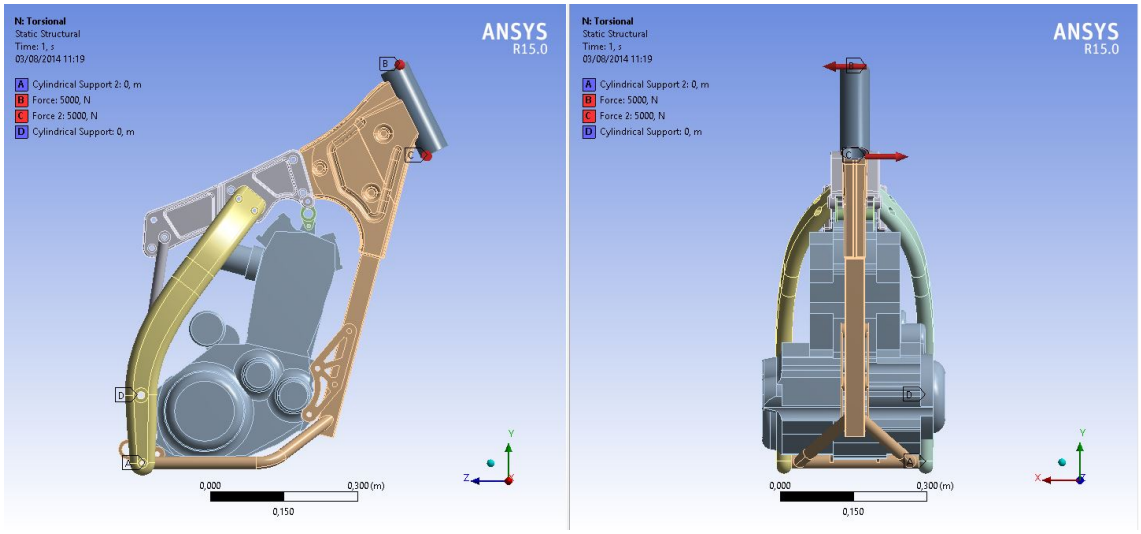

Figure 4.13: Case 5 parameters for the main frame introduced in *ANSYS® Workbench 15.0*

4.6.1.2 Swing-arm

The same principle was applied as before, only this time the swing-arm was the part to test. Again, cylindrical supports were used to restrain the movement. These were inserted on the connecting supports of the swing-arm, as seen in Figure 4.14. Two opposing loads of 3846,2 N were applied for the same reason as referred in Subsection 4.6.1.1. As the width of the swing-arm is 26 cm on the outside faces of the wheel mounting orifices, these loads translated an effective torsional moment of 1 kNm.

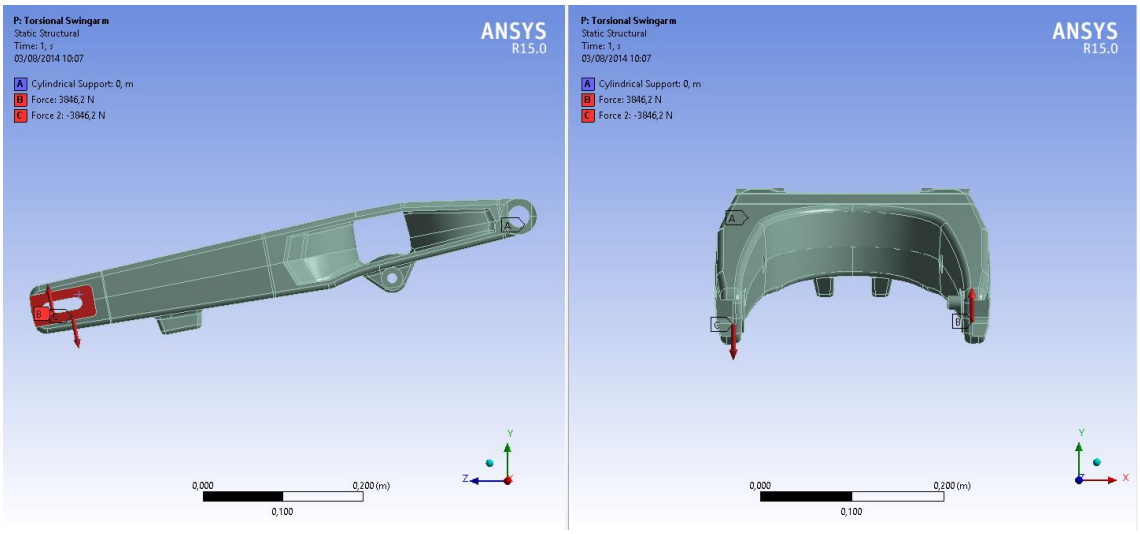

Figure 4.14: Case 5 parameters for the swing-arm introduced in *ANSYS® Workbench 15.0*

4.6.2 Results

4.6.2.1 Main Frame

The software used (*ANSYS® Workbench 15.0*) only retrieves as an output the total deformation values (displacement plus deformation of the parts), as shown in the Figures 4.15 and 4.16. For this reason an APDL Command was added to the results of both the main frame and swing-arm files (Appendix B).

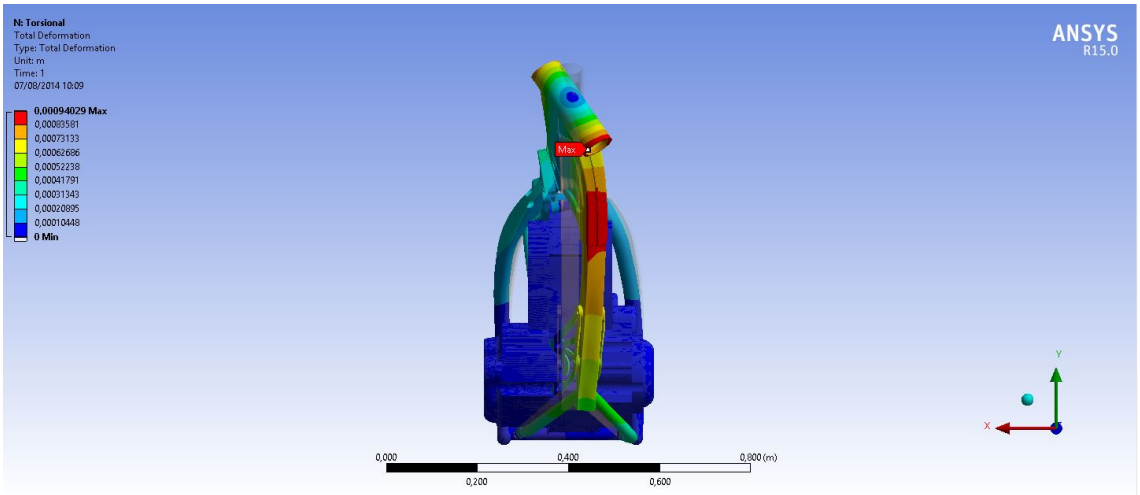

Figure 4.15: Torsional total deformation on the main frame extracted from *ANSYS® Workbench 15.0*

The maximum rotation was registered on the steering column, having a value of

0,48768º, which lead to a torsional stiffness of 2,05 kNm/º with the application of equation 4.2. This value lower to the minimum 3 kNm/º suggested by Vittore Cossalter.

To avert the low torsional stiffness, a reinforcement of the tube connecting the oil tank to the lower cradle can be applied. Also, internal or external ribs can be added to the oil tank as well as increasing the thickness of the wall or widening the whole oil tank. The connection with the backbone can also be adjusted to have not only the two metal flaps in between the backbone but also a little of the oil tank itself (either by extending the oil tank back or the backbone forward).

4.6.2.2 Swing-arm

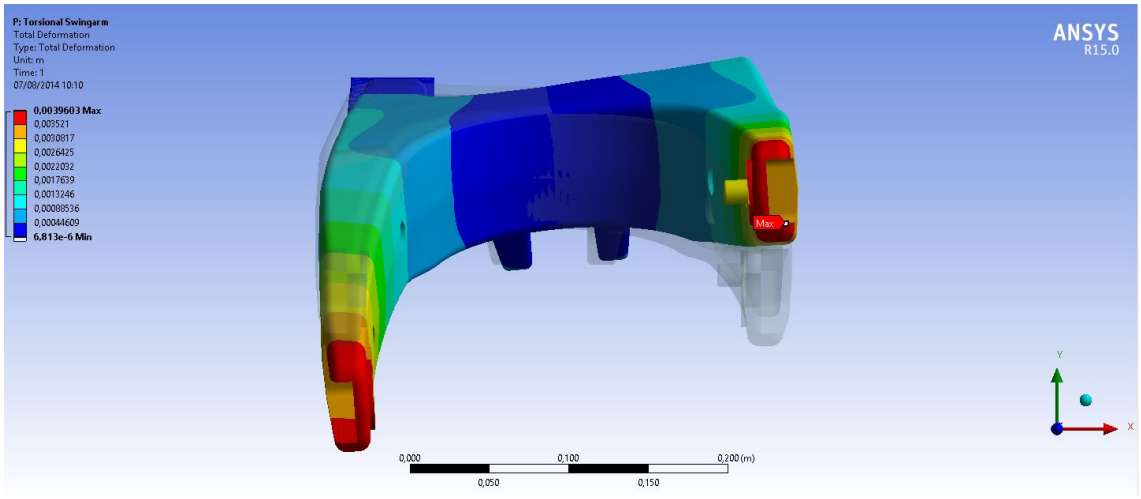

Figure 4.16: Torsional total deformation on the swing-arm extracted from *ANSYS® Workbench 15.0*

On the swing-arm the maximum rotation was 0,1871º. The stiffness calculated from it using equation 4.2 was 5,34 kNm/º, a value much higher than the 2 kNm/º referred in Vittore Cossalter's book. This might not be a bad thing since the motorcycle is intended to ride off-road and with a higher rigidity, the swing-arm will be able to take higher punishment.

Table 4.8: Torsional Stiffness Values Comparison

	Results	**Standard**
Main Frame	2,05	3-7
Swing-arm	5,34	1-2
	$kNm/^{o}$	$kNm/^{o}$

4.7 Case 6: Lateral Stiffness

The lateral stiffness, as well as the torsional stiffness, confers good road holding and handling if high enough. To evaluate the components and preform a comparison between the results and the Table 4.1 values a lateral load had to be applied to the components in study.

Table 4.9: Lateral Stiffness Values extracted from Table 4.1

Component	**Lateral** (kN/mm)
Main Frame	1-3
Swing-arm	0,8-0,16

4.7.1 Analysis Parameters

4.7.1.1 Main Frame

The main frame was constrained in the same manner as explained in the Subsection 4.6.1.1, but this time the load applied was 1 kN on the X axis direction (Figure 4.17).

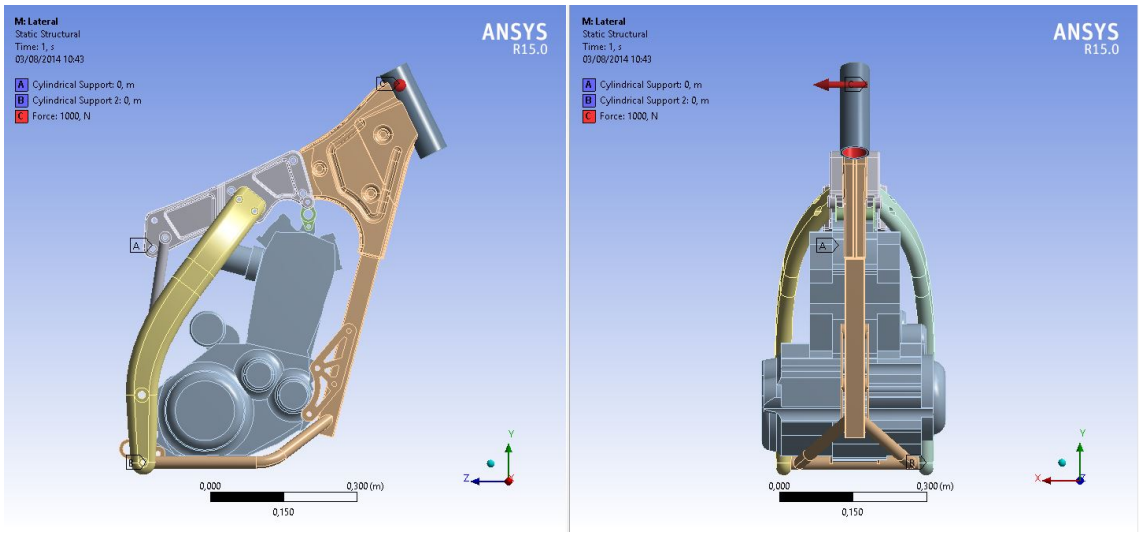

Figure 4.17: Case 6 parameters for the main frame introduced in *ANSYS® Workbench 15.0*

4.7.1.2 Swing-arm

As in the torsional stiffness case, the lateral stiffness was also analysed on the swing-arm. The restrains were the same as in Subsection 4.6.1.2. The loads were applied on the

rear wheel mounting orifices with a value of 500 N each, for a combined force of 1 kN (Figure 4.18).

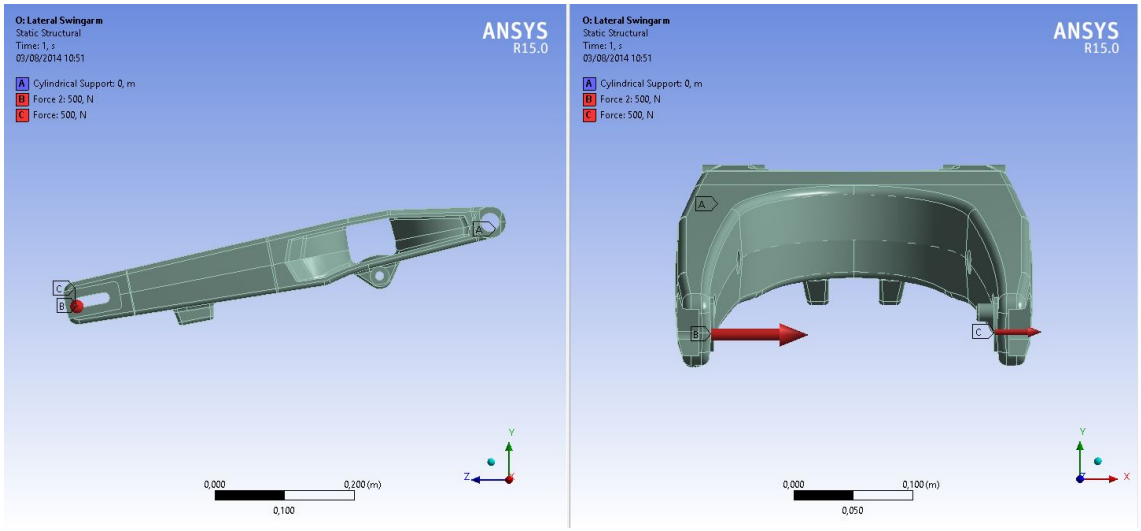

Figure 4.18: Case 6 parameters for the swing-arm introduced in *ANSYS® Workbench 15.0*

4.7.2 Results

4.7.2.1 Main Frame

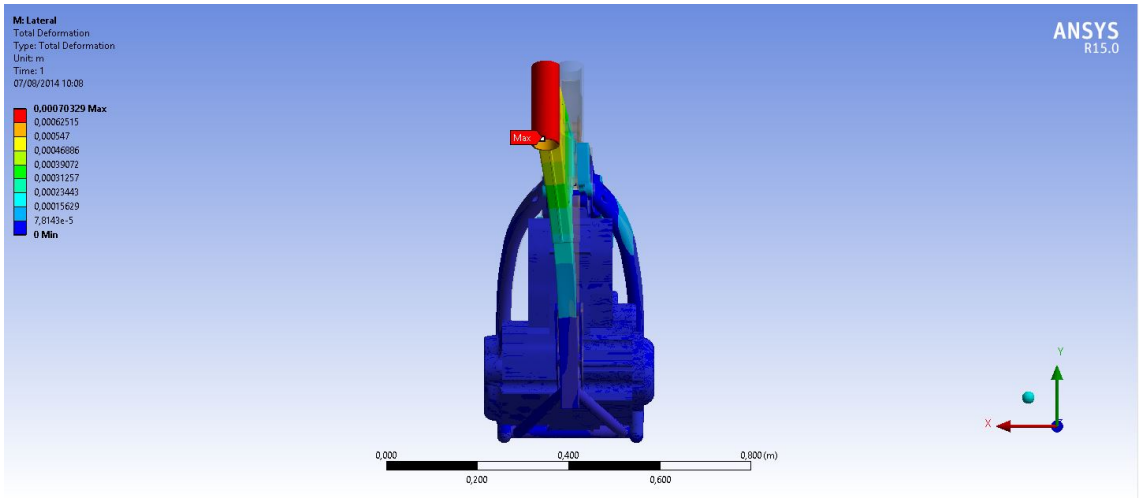

Figure 4.19: Lateral total deformation on the main frame extracted from *ANSYS® Workbench 15.0*

As well as in the case before the highest displacement plus deformation was measured in the steering column, having a value of 0,70329 mm. This value was considered to be

the displacement in order to simplify the calculations. Applying equation 4.1 a value of 1,42 kN/mm was calculated.

This value stands right in the middle of the standard lateral stiffness suggested for the main frame (1-3 kN/mm), leading to believe that the frame is stiff enough laterally.

4.7.2.2 Swing-arm

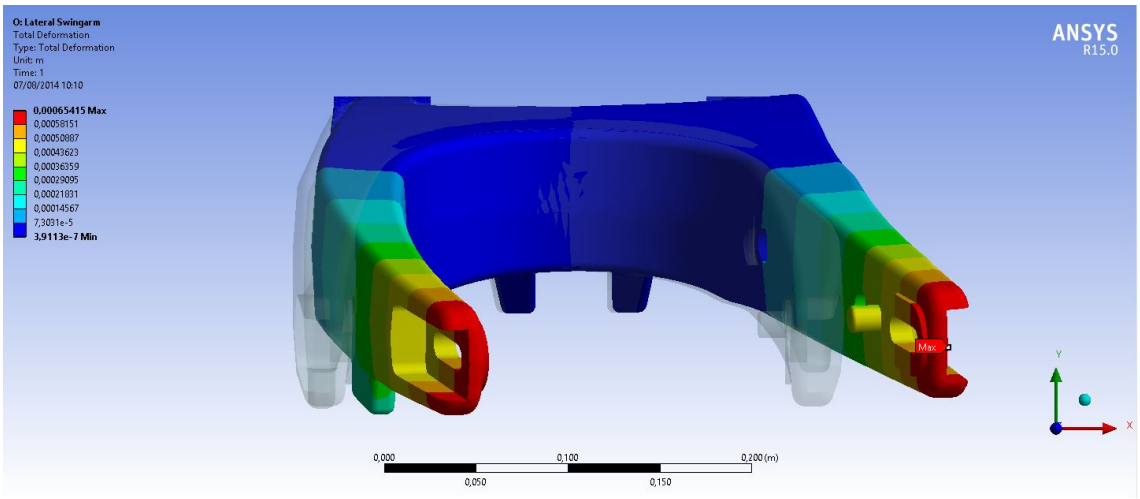

Figure 4.20: Lateral total deformation on the swing-arm extracted from *ANSYS® Workbench 15.0*

The swing-arm results show a maximum total deformation in *ANSYS® Workbench 15.0* of 0,61415 mm. Using equation 4.1, a value of 1,57 kN/mm was calculated for the lateral stiffness of the swing-arm.

As in the case before, the lateral stiffness calculated is much higher that the one suggested by Vittore Cossalter (0,8-0,16 kN/mm). This might be a good thing due to what was mentioned in the subsection 4.6.2.2, however, a road test should be done to ensure the comfort of the vehicle, as a too high stiffness may cause rider's discomfort.

Table 4.10: Lateral Stiffness Values Comparison

	Results	**Standard**
Main Frame	1,42	1-3
Swing-arm	1,53	0,8-0,16
	kN/mm	kN/mm

4.8 Case 7: Vertical Stiffness

4.8.1 Analysis Parameters

For the vertical stiffness, only the main frame had comparison values (Table 4.1), so just this one was analysed. As before, the main frame was constrained on the feet supports and on the swing arm connections to the main frame. The load this time was aligned with he direction of the steering column and had a magnitude of 1 kN (Figure 4.21).

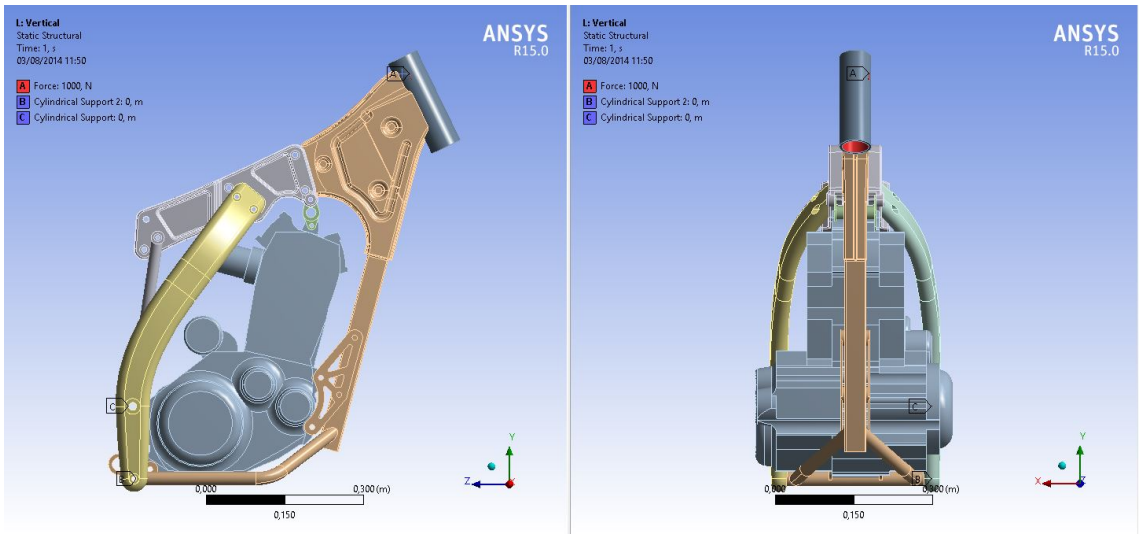

Figure 4.21: Case 7 parameters for the main frame introduced in *ANSYS® Workbench 15.0*

Table 4.11: Vertical Stiffness Values extracted from Table 4.1

Component	**Vertical** (kN/mm)
Main Frame	5-10

4.8.2 Results

The maximum total deformation read in *ANSYS® Workbench 15.0* was of 0,095864 mm. The equation 4.1 was applied and a value for the vertical stiffness of 10,43 kN/mm was obtained.

This value is a little over the maximum stiffness value specified in the book *Motorcycle Dynamics* but this most certainly will not lead to a problem.

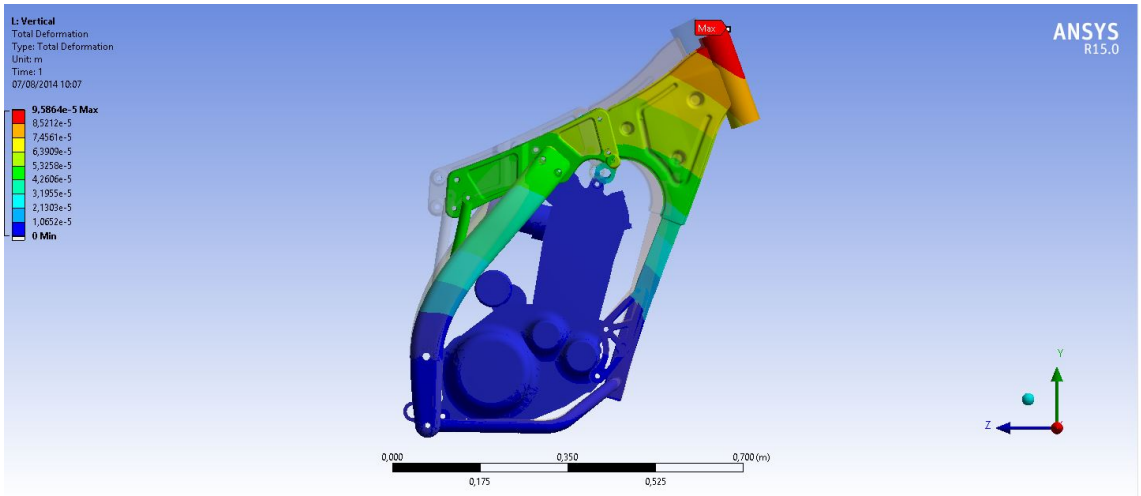

Figure 4.22: Vertical total deformation extracted from *ANSYS® Workbench 15.0*

Table 4.12: Vertical Stiffness Values Comparison

	Results	**Standard**
Main Frame	10,43	5-10
	kN/mm	kN/mm

4.9 Summary

This frame was well designed, however it has a few minor problems that can be easily overcome.

In the first part of the analysis it was possible to notice that, only in the landing with only the back wheel, the stresses were extremely high, as can be seen in Table 4.14. This may be due to considering the shock absorber rigid. Even so it needs some more attention and some suggestions were made to improve it.

Table 4.13: Maximum stress values

		Steel Parts	**Aluminium Parts**
Case 1	**Vertical**	217,86	87,236
	Rider aligned	113,4	63,468
Case 2	**Braking**	152,45	30,958
	Frontal impact	99,995	26,883
Case 3	**Landing back wheel**	819,62	387,5
Case 4	**Landing front wheel**	264,99	50,053
		MPa	*MPa*

The second part of the analysis was comprised of the comparison with the results values with the ones suggested by Vittore Cossalter in his *Motorcycle Dynamics* book.

In this part it was noticed that the main frame had values close to the standard ones. However, the torsional stiffness of the chassis studied is a little under the values specified. This may cause some discomfort or a poorer handling than the manufacturer wants. This problem was addressed with some suggestions on how to improve the performance on that point but no further analysis were made since it implied a major design change.

The swing-arm stiffness was a lot higher than the one suggested and, as said before (Subchapters 4.6.2.2 and 4.7.2.2), this should be addressed also as it may cause discomfort due to the high stiffness.

Table 4.14: Stiffness values comparison with the values suggested in *Motorcycle Dynamics*

		Main Frame		**Swing-arm**		
		Results	**Standard**	**Results**	**Standard**	
Case 5	**Torsional**	2,05	3-7	5,34	1-2	$kNm/^{o}$
Case 6	**Lateral**	1,42	1-3	1,53	0,8-0,16	kN/mm
Case 7	**Vertical**	10,43	5-10	–	–	kN/mm

Chapter 5

Modal Analysis

The ride comfort and handling of a motorcycle can make it stand out from the others. Being so, the modal analysis, is a great tool to achieve the comfort desired as the vibrations felt directly affect this.

The presence of vibrations usually leads to undesirable effects such as movement amplitudes that exceed the predicted in the project and may affect the good functioning of the equipment, resonance frequencies may be reached and may originate high deformation or stresses that can lead the equipments to rupture and may also lead to the early wear of the components. [29]

To avert this situation a simple modal analysis of this frame was conducted. This analysis was based on the thesis written by António Pedro Paiva for AJP Motos in 2012. [30] Also, as the prototype is not ready to be tested, a comparison with a previous model of the company, the one used in António Pedro Paiva's thesis, was used. The model was the chassis of the AJP Motos PR4 and the values were obtained through an experimental analysis.

As in the aforementioned thesis, the analysis will be made first on the separate parts of the frame and only afterwards on the full frame.

The numerical analysis, as before, will be made using the software *ANSYS® Workbench 15.0*. All the parts were not constrained, so that a free-free condition is verified.

5.1 Lower Frame

5.1.1 Analysis Parameters

The first part to be analysed was the lower frame, or as referred in the subsection 3.1.1, the part comprised of the oil tank, steering column and engine cradle.

A new mesh was applied to this part and the numerical analysis was run with an interval ranging from 1 to 1000 Hz, with the end of finding the six first modal modes.

Figure 5.1: Lower frame mesh for the modal analysis generated by *ANSYS® Workbench 15.0*

5.1.2 Results

Table 5.1: Natural vibration frequencies for the lower frame extracted from *ANSYS® Workbench 15.0* and comparison with the ones obtained for PR4 [30]

Mode	Natural Frequencies	Comparison Frequencies	Relative Deviations
1	73,804	83,5	11,6
2	92,313	139	33,6
3	136,29	226	39,7
4	238,95	286	16,4
5	250,02	407	38,6
6	458,73	586	21,7
	Hz	*Hz*	*%*

It is possible to see that the natural frequencies are lower than the comparison frequencies. This may be due to the frame being tested having a bigger structure than the PR4 frame. Another reason may be due to the lack of reinforcement in the frame, because

it can be seen that the comparison model was reinforced near the steering column and in the lower cradle (Figure 5.2). Even so, the results are not that far of but they begin to be farther apart the higher the mode.

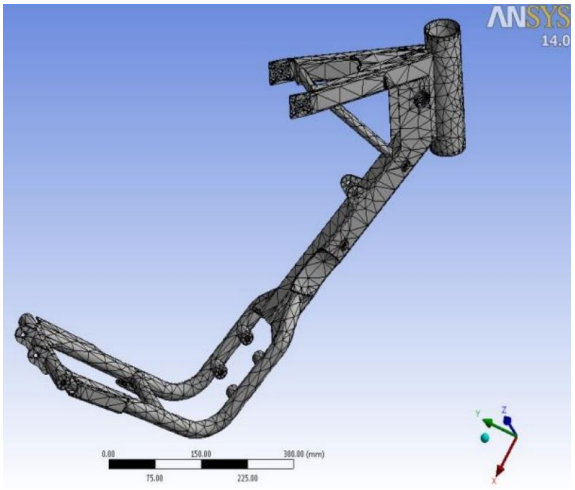

Figure 5.2: PR4 lower frame used for comparison [30]

5.2 Lateral Beams and Backbone

5.2.1 Analysis Parameters

As in the previous part, the six first modal modes were calculated using *ANSYS® Workbench 15.0* in an interval from 1 to 1000 Hz.

A new mesh was also generated for this part as it was comprised from half the backbone and the right lateral beam.

Only the right lateral beam is presented here, since both sides are symmetric.

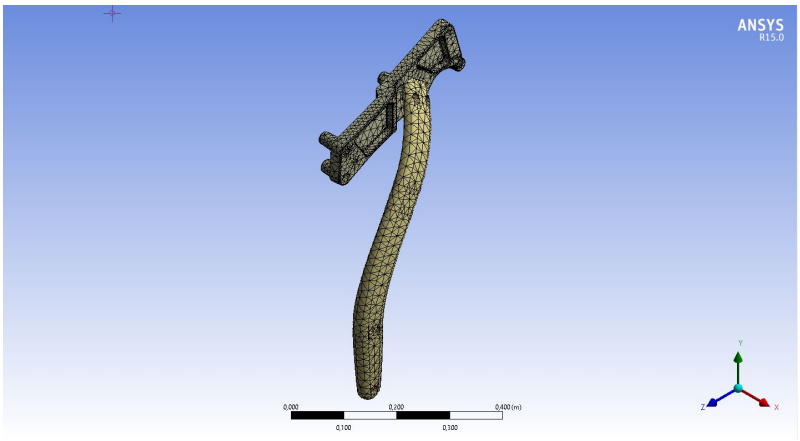

Figure 5.3: Right lateral beam mesh for the modal analysis generated by *ANSYS® Workbench 15.0*

5.2.2 Results

Table 5.2: Natural vibration frequencies for the right lateral beam extracted from *ANSYS® Workbench 15.0* and comparison with the ones obtained for PR4 [30]

Mode	Results Frequencies	Comparison Frequencies	Relative Deviations
1	241,29	304,5	20,8
2	315,3	383	17,7
3	358,72	702	48,9
4	729,34	917	20,5
5	894,13	1096	18,4
6	947,08	1218,5	22,2
	Hz	*Hz*	*%*

It is possible to see that the natural frequencies are quite close but still a little bit lower. There is, however, two natural frequencies that are quite close to each other (mode 2 and mode 3 frequencies). This creates what looks like a repeated frequency, since the modes after that present frequencies that have around the same value as the comparison frequencies of the previous modes. This, however, could not be proved as the modes for the lateral beams were not presented in António Paiva's thesis.

It should also be noted that the lateral beam used for comparison (Figure 5.4) has more rigidity due to the inclusion of the shock absorber supports, while the model in study has the supports separated from the side beams, since these are connected through the use of a rod and are kept in place by the engine and the swing-arm.

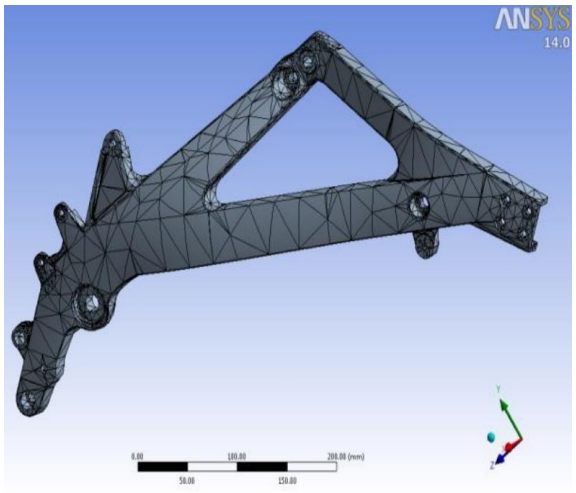

Figure 5.4: PR4 right lateral beam used for comparison [30]

5.3 Main Frame

5.3.1 Analysis Parameters

The next in line was the analysis of the main frame. Again a new mesh was generated since there were a few minor changes to the model, such as the removal of the swing-arm connecting rods support. It should be noted that the suspension rods are also not included in the analysis. These are to be mounted in between the rear engine mount and the swing-arm, thus, without these parts, the suspension rods would swing freely and would create frequencies with lower magnitudes due to the pendulum movement of the rods.

The analysis was once again run in an interval from 1 to 1000 Hz.

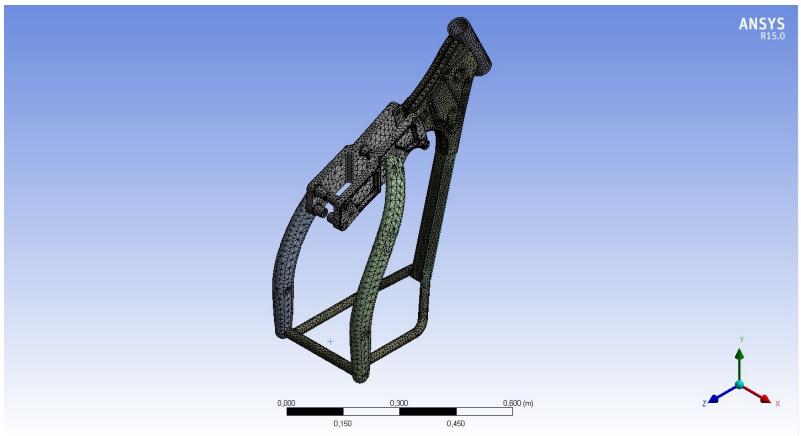

Figure 5.5: Main frame mesh for the modal analysis generated by *ANSYS® Workbench 15.0*

5.3.2 Results

Table 5.3: Natural vibration frequencies for the main frame extracted from *ANSYS® Workbench 15.0* and comparison with the ones obtained for PR4 [30]

Mode	Results Frequencies	Comparison Frequencies	Relative Deviations
1	120,51	214	43,7
2	180,8	271	33,3
3	237,04	281	15,6
4	273,31	288	5,1
5	294,57	327	9,9
6	370,82	–	–
	Hz	*Hz*	*%*

As it is possible to see in table 5.4, the values of the natural frequencies are, again, lower than the reference values. The values, however, approach the latter the higher the mode. This indicates that the new chassis probably has the same performance and problems as the PR4 chassis.

The lower values for the frequencies are probably due to the lack of the suspension connecting rods. This because the beams that are instead of those in the AJP Motos PR4 chassis (Figure 5.6) confer an higher structural rigidity to the frame.

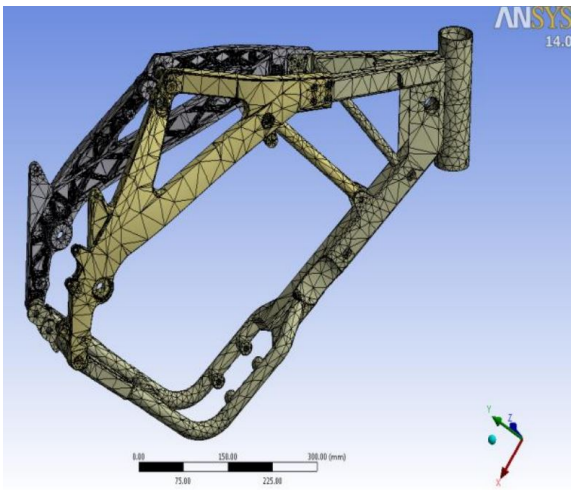

Figure 5.6: PR4 main frame used for comparison [30]

The modes correspondent to the main frame natural frequencies are registered in figure 5.9.

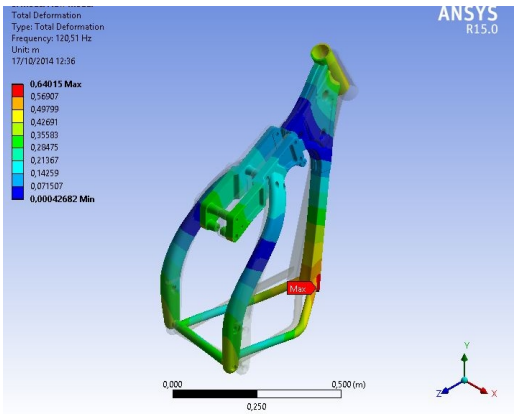

(a) Mode 1 - PR7

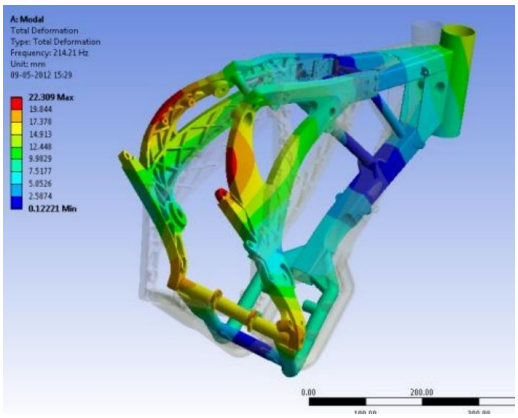

(b) Mode 1 - PR4

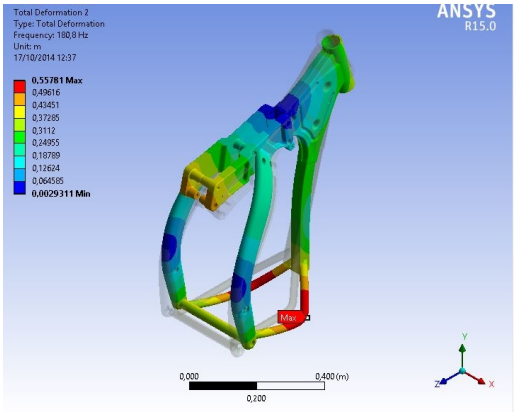

(c) Mode 2 - PR7

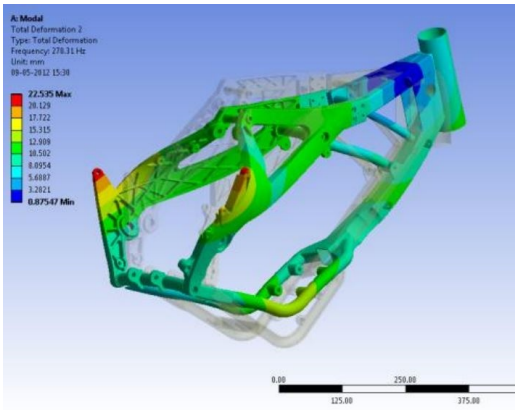

(d) Mode 2 - PR4

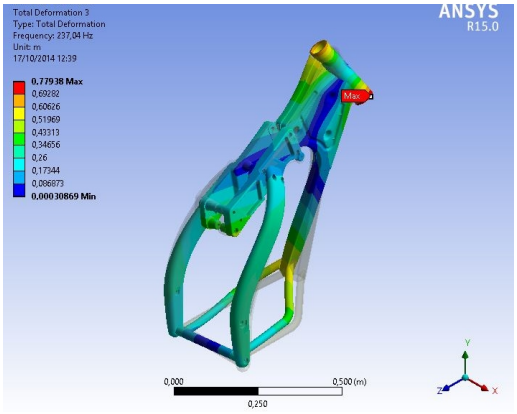

(e) Mode 3 - PR7

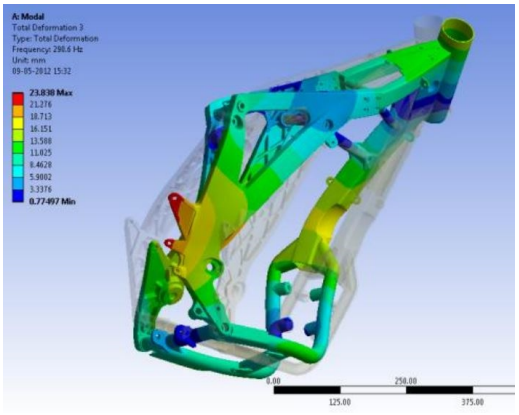

(f) Mode 3 - PR4

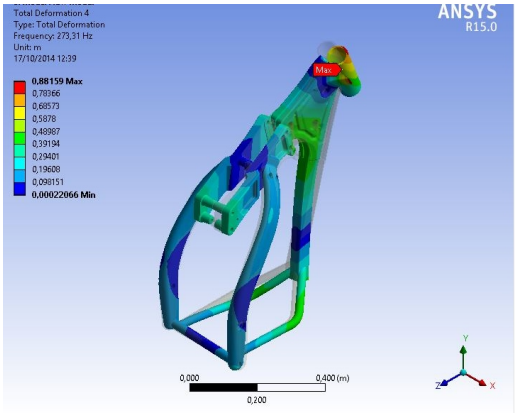

(g) Mode 4 - PR7

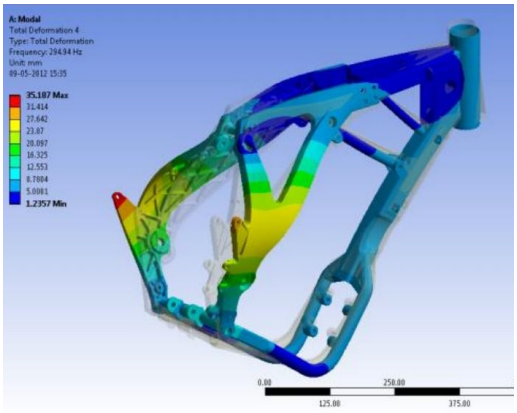

(h) Mode 4 - PR4

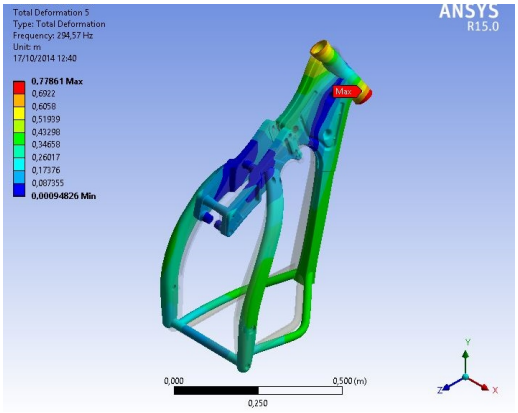

(i) Mode 5 - PR7

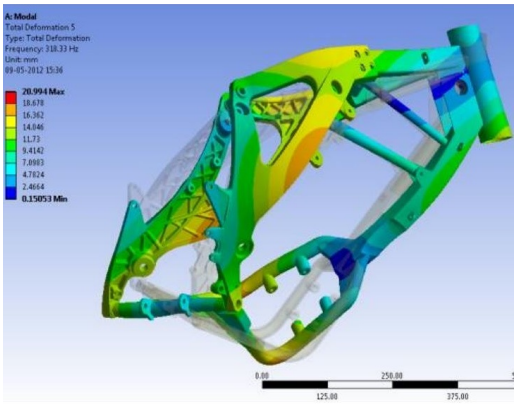

(j) Mode 5 - PR4

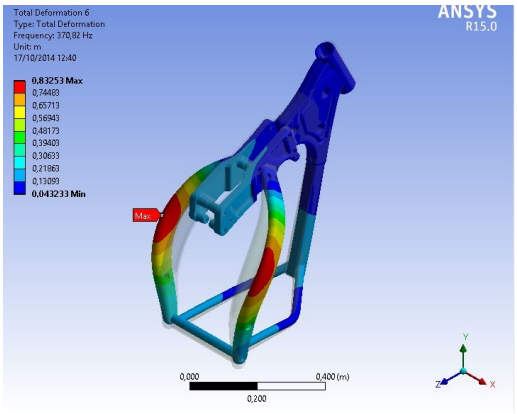

(k) Mode 6 - PR7

Figure 5.7: Natural vibration modes for the main frame extracted from *ANSYS® Workbench 15.0* and comparison with PR4 results

5.4 Swing-arm

5.4.1 Analysis Parameters

The swing-arm was not studied in António Paiva's thesis [30], to which the results are being compared to. Even so, as the swing-arm is the direct connection of the wheels to the main frame, it should be analysed so that no undesirable vibrations are felt or transmitted through this mean to the main frame.

The swing-arm was re-meshed and was subjected to the numerical modal analysis in *ANSYS® Workbench 15.0* within the values of 1 and 2000 Hz and the first six modes and natural frequencies were extracted.

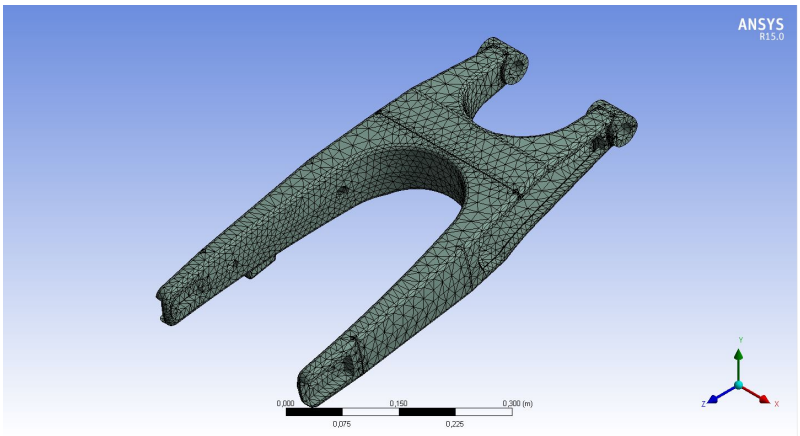

Figure 5.8: Swing-arm mesh for the modal analysis generated by *ANSYS® Workbench 15.0*

5.4.2 Results

Table 5.4: Natural vibration frequencies for the swing-arm extracted from *ANSYS® Workbench 15.0*

Mode	Results Frequencies
1	259,57
2	292,73
3	540,18
4	709,03
5	1000,1
6	1041,1
	Hz

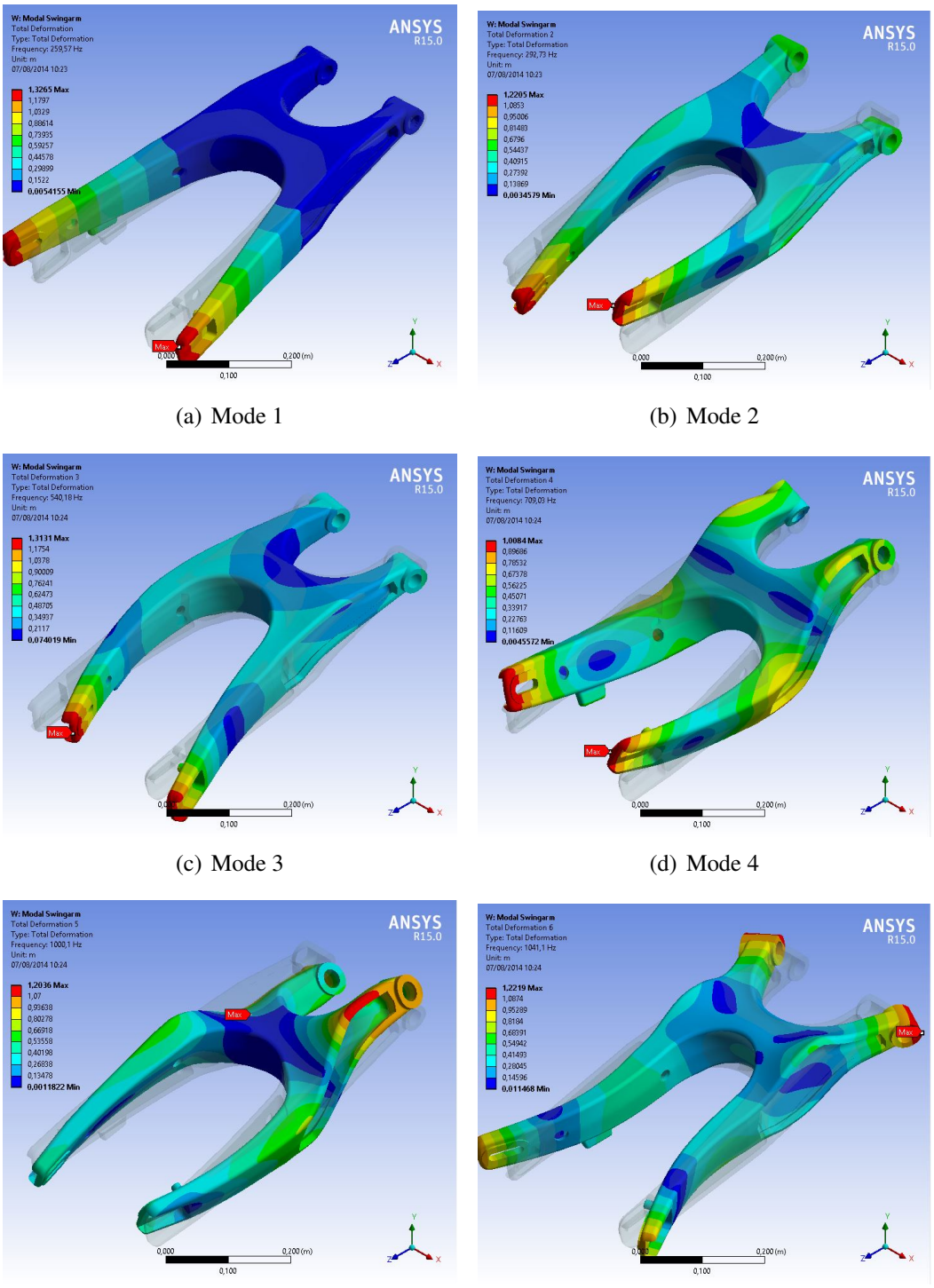

(a) Mode 1 (b) Mode 2

(c) Mode 3 (d) Mode 4

(e) Mode 5 (f) Mode 6

Figure 5.9: Natural vibration modes for the swing-arm extracted from *ANSYS® Workbench 15.0*

As it is possible to see, the natural frequencies are quite high and the swing-arm should

not pose a problem with vibrations, however no comparison was possible to be made. To validate this results an experimental analysis should be performed.

5.5 Summary

It was possible to observe that the natural frequencies are not that far off and that the discrepancies are probably, mainly, due to the shock absorber connecting rods.

Even so, the lower cradle should be addressed to elevate the first modes frequencies as to create a more comfortable ride.

The main frame's lower natural frequencies should be due to the missing shock absorber connecting rods, as said before. However, it can not be taken as certain and thus an analysis with the full frame and the shock absorbers and dampers in place should be made.

Chapter 6

Conclusions and Future Work

6.1 Conclusions

The given problem requires a complete analysis of the frame and the loads one usually is submitted when the motorcycle is used. This, however, is a complex problem due to the interaction of the numerous different components. Therefore, the problem was simplified with the consideration of some parts as rigid and the welded parts as a single part.

Also, with little or no information about the critical loads a motorcycle should be able to bear (for the analysis set up), critical loads were considered to have the magnitude equal to three times the weight of the system (rider plus motorcycle). Only with this decision was possible to analyse the given problem and comment on it.

The connections between the different parts as well as its function was understood in a way that it could, as closely as possible, translate its functioning on the motorcycle.

For the proper analysis to be performed, a suitable mesh had to be generated. This was done with the attention of providing a smaller mesh on and around the places where the critical points were suspected to be, with further adjustments when needed.

Different sets of cases were created and studied, including three stiffness tests that could be compared to standard values, and commented with the additional suggestions for improvement when needed.

Additionally a modal analysis was performed for the structure and the values were compared to others previously tested on another motorcycle.

6.1.1 Results

As far as results go, the frame performed well. Having, however, two points of major concern.

The first point discovered was the extreme solicitation on the swing-arm connecting rod supports as well as the connecting rods themselves when the motorcycle lands from a jump only with the back wheel. The most concerning situation was the first one due to the high stresses registered in that point. The situation was averted proposing a simple design change that halves the stresses in the said part. The other situation was considered to be the result of considering the rear shock absorber rigid.

The second concerning point was the lower than average values for the torsional stiffness of the frame. To contour this situation some suggestions were made but no actual tests were done since it implied major design changes.

For the modal analysis, the results were considered to be close to the ones they were compared to. The discrepancies between both were attributed to the different construction way of the frames, as one has a single part connecting the front of the frame to the lower frame and rear suspension that makes a closed contour and the other presents the same connection with three parts and closing the contour. This makes the latter chassis more difficult to test as it needs more parts and the connections between them are more complex.

6.1.2 Critical Analysis

As this thesis was proceeding its course, many problems arose. Some of them were possible to overcome, while others were definite.

The first problem encountered was related with the literature available about this type of problems. Usually the development of new vehicles as well as their analysis and tests are kept secret and only available to the company. For this reason, the only completely reliable information collected came from books being the majority of the other literature works such as this one.

In the second phase, after receiving the model, it had to be reworked so that it was possible to run a finite element method analysis. The parts had to be realigned and some of them redrawn so that all the components fitted well without any overlapped pieces. This process was not as swift as it could have been since the author did not have, at the time, the knowledge and experience to make the decisions needed. This, however, improved the author's decision skills.

A prototype experimental test was also on the minds of both the author and supervisor but the time needed and the costs associated with the prototyping process made it impossible to be achieved. This way it was not possible to prove the results and offer what would have been a more accurate analysis.

6.2 Future Work

On a first approach the prototype should be experimentally tested in the laboratory to prove the results and fine tune the analysis. After this, a road test should be preformed and counter the results obtained from the numerical analysis with the practical results of the test.

The rigid parts should also be replaced with the models or constraints with the same properties as the parts to be used in the motorcycle, both in the static numeric analysis and in the modal numeric analysis. This would give a better insight of how the motorcycle will preform on the road and more improvements can be made.

After finishing all the points suggested before, the results should be again compared to the prototype to ensure that the model represents the actual motorcycle to its fullest so that any changes can be tested using only the computer without the intervention of any other physical prototypes.

Appendix A

Results from the pre-analysis extracted from *Solidworks*®

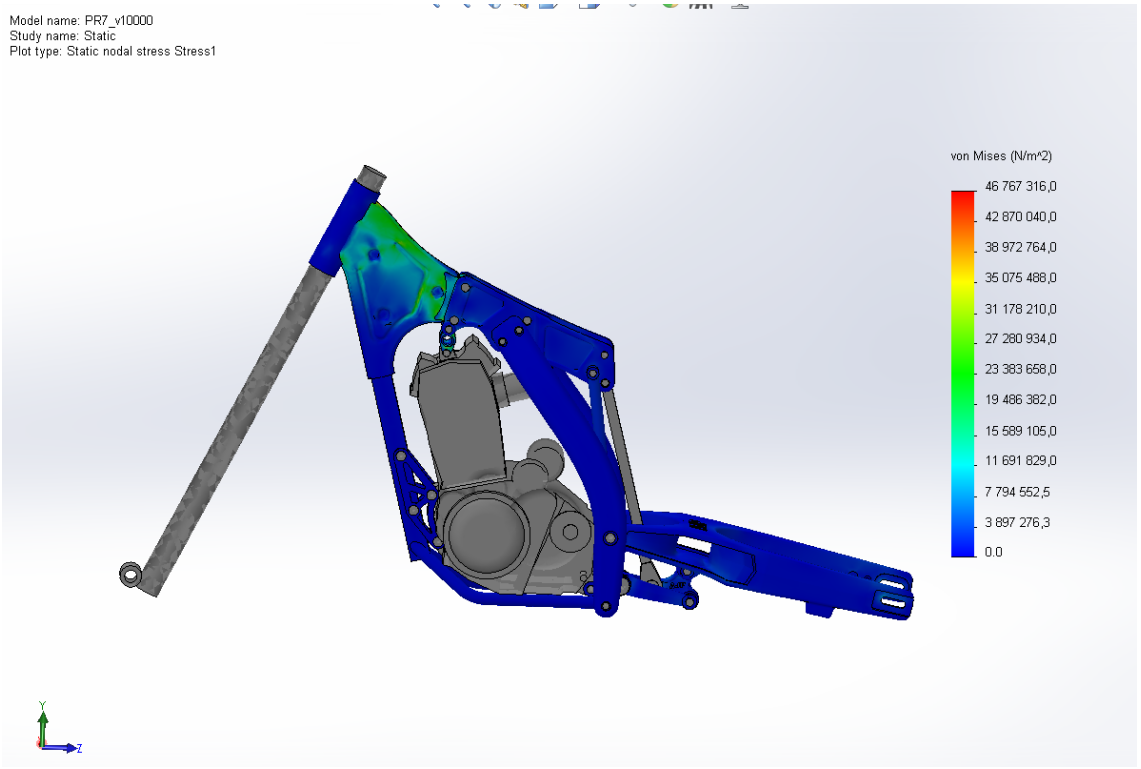

(a) Von Mises Stress

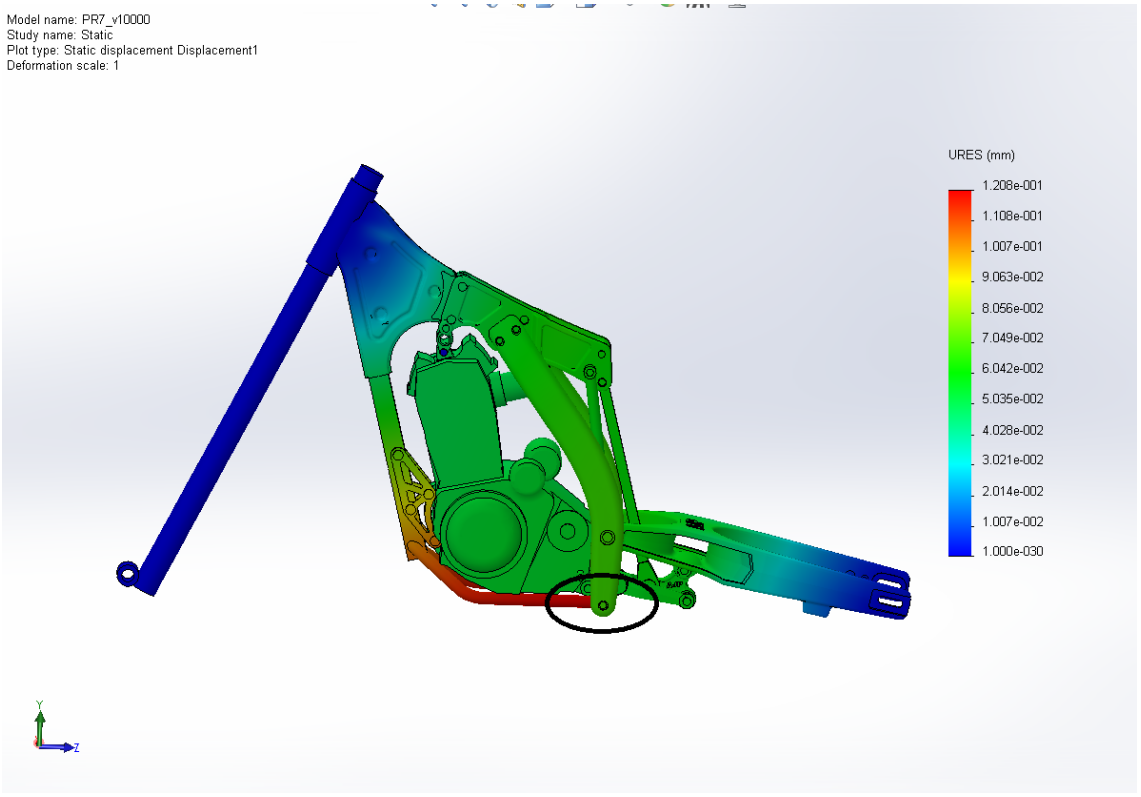

(b) Displacements

Figure A.1: Results from the pre-analysis extracted from *Solidworks®*

Appendix B

APLD Commands inserted in *ANSYS*® *Workbench 15.0* to retrieve the rotation in the torsional analysis

! Commands inserted into this file will be executed immediately after the ANSYS /POST1 command.

! Active UNIT system in Workbench when this object was created: Metric (m, kg, N, s, V, A)
! NOTE: Any data that requires units (such as mass) is assumed to be in the consistent solver unit system.
! See Solving Units in the help system for more information.

RSYS,12
my_ rotx=ROTX(Measure_ Pilot)*57.29577951
my_ roty=ROTY(Measure_ Pilot)*57.29577951
my_ rotz=ROTZ(Measure_ Pilot)*57.29577951

Appendix C

Market Opponent Models

C.1 Yamaha XT660Z Ténéré

Figure C.1: Yamaha XT660Z Ténéré [26]

Table C.1: Yamaha XT660Z Ténéré Technical Specifications [26]

Engine

Engine Type	Single Cylinder
Displacement	660 cc
Bore x Stroke	100.0 mm x 84.0 mm
Compression Ratio	10.0 : 1
Maximum Power	35.0 kW (46.9 hp) @ 6000 rpm
Maximum Torque	58.0 Nm @ 5500 rpm
Lubrication System	Dry Sump
Clutch Type	Wet, Multiple-disc Coil Spring
Carburettor	Electronic Fuel Injection
Ignition System	TCI
Starter System	Electric
Transmission System	Constant Mesh, 5 Speed
Final Transmission	Chain

Chassis

Frame	Steel tube diamond shape
Front suspension system	Telescopic forks
Front travel	210 mm
Caster angle	28°
Trail	113 mm
Rear suspension system	Linked mono-shock with spring pre-load adjustment
Rear travel	200 mm
Front brake	Hydraulic dual disc, ø298 mm
Rear brake	Hydraulic single disc, ø245 mm
Front tyre	90/90-21 M/C
Rear tyre	130/80-17 M/C

Dimensions

Overall length	2.246 mm
Overall width	896 mm
Overall height	1.477 mm
Seat height	896 mm
Wheel base	1.500 mm
Minimum ground clearance	260 mm
Wet weight (including full oil and fuel tank)	208,5 kg
Fuel tank capacity	23 litres
Oil tank capacity	2,9 litres

C.2 BMW G650 GS

Figure C.2: BMW G650 GS [31]

Table C.2: BMW G650 GS Technical Specifications [31]

Engine

Engine Type	Water-cooled, single-cylinder 4-stroke engine, four valves, two overhead camshafts, dry sump lubrication
Displacement	652 cc
Bore x Stroke	100 mm x 83 mm
Compression Ratio	11.5 : 1
Maximum Power	35 kW (48 hp) at 6,500 rpm (output reduction to 25 kW (34 hp) at 6,500 rpm possible)
Maximum Torque	60 Nm at 5,000 rpm (with output reduction: 47 Nm at 4,500 rpm)
Mixture control / engine managemen	Electronic intake pipe injection / BMW engine management, twin-spark ignition
Clutch Type	Multiple-disc clutch in oil bath, mechanically operated
Emission control	Closed-loop 3-way catalytic converter, emission standard EU-3

Performance / fuel consumption

Maximum speed	approx. 170 km/h (with output reduction: approx. 145 km/h)
Fuel consumption per 100 km at constant 90 km/h	3.2 l
Fuel consumption per 100 km at constant 120 km/h	4.3 l
Fuel type	Unleaded regular, minimum octane rating 91 (RON)

Electrical system

Alternator	three-phase alternator 400 W
Battery	12 V / 12 Ah

Power transmission

Clutch	Multiple-disc clutch in oil bath, mechanically operated
Gearbox	Constant mesh 5-speed gearbox integrated into crankcase
Drive	Endless O-ring chain with shock damping in rear wheel hub

Chassis / brakes

Frame	Bridge-type steel section frame with bolted-on rear section
Front wheel location / suspension	Telescopic fork, ø41 mm, fork stabiliser
Rear wheel location / suspension	Box-section steel dual swing-arm, central spring strut operated by lever system, spring pre-load hydraulically adjustable (continuously variable) at handwheel, rebound damping adjustable
Suspension travel front / rear	170 mm / 165 mm (lowered suspension 140 mm / 130 mm)
Wheelbase	1.477 mm
Castor	113 mm
Steering head angle	61,9°
Wheels	Cast aluminium
Rim, front	2,50 x 19"
Rim, rear	3,50 x 17"
Tyres, front	110/80 R19 59V
Tyres, rear	140/80 R17 69V
Brake, front	Single disc, diameter 300 mm, double-piston floating caliper
Brake, rear	Single disc, diameter 240 mm, single-piston floating caliper
ABS	Standard

Dimensions / weights

Length	2.165 mm
Width (incl. mirrors)	920 mm
Height (excl. mirrors	1.390 mm
Seat height, unladen weight	800 mm (with motorcycles accessories or –equipment variable heights available between 770 mm and 840 mm)
Inner leg curve, unladen weight	1810 mm (with motorcycles accessories or –equipment variable heights available between 1750 mm and 1890 mm)
Unladen weight, road ready, fully fuelled 1)	192 kg
Dry weight 2)	175 kg
Permitted total weight	380 kg
Payload (with standard equipment)	188 kg
Usable tank volume	14.0 l
Reserve	approx. 4.0 l

C.3 KTM 690 Enduro R

Figure C.3: KTM 690 Enduro R [32]

Table C.3: KTM 690 Enduro R Technical Specifications [32]

Engine

Engine Type	Single-cylinder, 4-stroke, spark-ignition engine, liquid-cooled
Displacement	690 cc
Bore x Stroke	102.0 mm x 84.5 mm
Maximum Power	49 kW (66 hp)
Primary gear ratio	36:79
Primary gear ratio	15:45
Lubrication System	Pressure circulation lubrication with two rotor pumps
Clutch Type	APTC^{TM} Anti-hopping clutch in oil bath / hydraulically operated
Ignition System	Contactless, controlled, fully electronic ignition system with digital ignition timing adjustment
Starter System	Electric starter, automatic decompressor
Transmission System	6-speed, claw shifted

Chassis

Frame	Tubular space frame made from chrome molybdenum steel, powder-coated
Fork	WP Suspension 4860 D48/26 MA
Shock absorber	WP Suspension 4618 with Pro-Lever linkage
Suspension travel front	250 mm
Suspension travel rear	250 mm
Brake system front	Disc brake with two-piston brake caliper, floating
Brake system rear	Disc brake with single-piston brake caliper, floating
Brake discs - diameter front	300 mm
Brake discs - diameter rear	240 mm
Chain	5/8 x 1/4" X-Ring
Steering head angle	63^{o}
Wheel base	1.504$\pm$15 mm
Ground clearance (unloaded)	280 mm
Seat height (unloaded)	910 mm
Total fuel tank capacity approx.	12 l, Unleaded premium fuel (95 RON)
Weight without fuel approx.	139 kg

References

[1] TMW TotalMotorcycle.com. The history and future of motorcycles and motorcycling - from 1885 to the future, electric, gas, diesel, hybrid motorcycles. **URL:** http://www.totalmotorcycle.com/future.htm1800s, 2014. Last Accessed 2014.07.10.

[2] Daimler Motorcycle. 1867 roper steam velocipede. **URL:** http://daimlermotorcycle.com/Roper.htm, 2012. Last Accessed 2014.07.03.

[3] William Harris. Motorcycle history. **URL:** http://auto.howstuffworks.com/motorcycle6.htm, 2014. Last Accessed 2014.07.03.

[4] Mark Whiting. The evolution of motorcycle design. **URL:** http://www.andrew.cmu.edu/org/CDL/research/Harley/History.htm, 2005. Last Accessed 2014.07.04.

[5] Autoviva. Daimler reitwagen. **URL:** http://www.autoviva.com/reitwagen/version/28602, 2010. Last Accessed 2014.07.04.

[6] Miguel Ângelo Nogueira da Costa Oliveira. Validação estrutural de um novo conceito de chassis de motociclo, 2009.

[7] Ellen Hall. A brief history of the motorcycle: From boneshakers to superbikes. **URL:** http://blog.esurance.com/a-brief-history-of-the-motorcycle-from-boneshakers-to-superbikes, 2013. Last Accessed 04.07.2014.

[8] Indian Motorcycle. Indian motorcycle timeline. **URL:** http://www.indianmotorcycle.com/en-us/stories/history, 2014. Last Accessed 2014.07.04.

[9] ChickGeek. Wwi harley-davidson. **URL:** http://chickgeek.org/wwi-harley-davidson/, 2013. Last Accessed 2014.07.07.

[10] ART Motorcycle Training Ltd. Motorcycle history in the uk and around the world. **URL:** http://www.artmotorcycletraining.co.uk/motorcycle_history.htm, 2014. Last Accessed 2014.07.08.

[11] Corpses From Hell. First ever honda motorcycle. model d the "dream". **URL=** http://corpsesfromhell.blogspot.pt/2009/10/

first-ever-hona-motorcycle-model-d.html, 2009. Last Accessed 2014.07.14.

[12] Basem Wasef. Chassis definition - the meaning of motorcycle chassis. **URL:** http://motorcycles.about.com/od/motorcycleglossary/g/chassis.htm, 2014. Last Accessed 2014.07.10.

[13] Super Streetbike. Motorcycle frames explained - the frame game. **URL:** http://www.superstreetbike.com/motorcycle-frames-explained-frame-game, 2009. Last Accessed 2014.07.14.

[14] Tony Foale. *Motorcycle Handling and Chassis Design: The Art and Science*. 2002.

[15] Derek J. Noce. *The engineering process for the design of a motorcycle chassis and suspension*. M.s.m.e., 2012. Copyright - Copyright ProQuest, UMI Dissertations Publishing 2012.

[16] Types of motorcycle frames. **URL:** http://pt.scribd.com/doc/89334946/Types-of-Motorcycle-Frames, 2014. Last Accessed 2014.07.22.

[17] Ltd Kawasaki Heavy Industries. Z800: Kawasaki motorcycle & engine company. **URL:** http://www.kawasaki-cp.khi.co.jp/mcy/street/14_zr800abcd_essence_2_e.html?page=4, 2013. Last Accessed 2014.07.23.

[18] Christine Harrell. Types of motorcycle frames. **URL:** http://motorbikeclaims.org.uk/articles/256/1/Types-of-Motorcycle-Frames/Page1.html, 2008. Last Accessed 2014.07.26.

[19] Jason Cormier. Norton p86 750 challenge - norton's last gasp. **URL:** http://www.odd-bike.com/2013/02/norton-p86-750-challenge-nortons-last.html, 2013. Last Accessed 2014.07.26.

[20] Tom Niemela and Bob Schwarz. What is dualsporting? **URL:** http://www.blackdogdualsport.com/WhatisDualsporting.htm, 1994. Last Accessed 2014.07.09.

[21] Kevin Duke. 2006 adventure touring comparo. **URL:** http://www.motorcycle-usa.com/12/650/Motorcycle-Article/2006-Adventure-Touring-Comparo.aspx, 2006. Last Accessed 2014.07.08.

[22] Mike McNessor. 1980 bmw r80 g/s. **URL:** http://www.hemmings.com/hmn/stories/2010/10/01/hmn_feature11.html, 2013. Last Accessed 2014.07.08.

[23] AJP Motos. Ajp motos - enduring experience. **URL:** http://www.ajpmotos.pt, 2012. Last Accessed 2014.07.21.

[24] G. R. Liu and S. S. Quek. *The Finite Element Method: A Practical Course*. 2003.

[25] Álvaro F. M. Azevedo. *Método dos Elementos Finitos*. Faculdade de Engenharia da Universidade do Porto, 2003.

[26] Yamaha. Xt660z tenere. **URL:** http://www.yamaha-motor.eu/eu/products/motorcycles/adventure/xt660z.aspx, 2014. Last Accessed 2014.07.30.

[27] Vittore Cossalter. *Motorcycle Dynamics*. 2nd edition edition, 2006.

[28] Mikel Burgui Oyaga and Alfredo Ursúa Rubio. Analysis and design of a motorbike chassis, 2011.

[29] José Dias Rodrigues. *Apontamentos de Vibrações de Sistemas Mecânicos*. 2013.

[30] António Pedro Dinis Paiva. Estudo de vibrações num motociclo, 2012.

[31] BMW Motorrad. Bmw motorrad international. **URL:** http://www.bmw-motorrad.com, 2014. Last Accessed 2014.08.27.

[32] KTM. Ktm 690 enduro r 2014. **URL:** http://www.ktm.com/pt/enduro/690-enduro-r-eu, 2014. Last Accessed 2014.08.27.